BBA - Molecular Cell Research 1866 (2019) 486–503

Contents lists available at ScienceDirect

BBA - Molecular Cell Research

journal homepage: www.elsevier.com/locate/bbamcr

Protease-activated receptor 2 induces migration and promotes Slug-mediated epithelial-mesenchymal transition in lung adenocarcinoma cells

Chung-Che Tsai[a], Yu-Ting Chou[b,c], Hua-Wen Fu[a,c,*]

[a] Institute of Molecular and Cellular Biology, National Tsing Hua University, Hsinchu 30013, Taiwan, ROC
[b] Institute of Biotechnology, National Tsing Hua University, Hsinchu 30013, Taiwan, ROC
[c] Department of Life Science, National Tsing Hua University, Hsinchu, 30013, Taiwan, ROC

ARTICLE INFO

Keywords:
PAR2
EMT
ERK1/2
β-Arrestin
Slug
Lung adenocarcinoma

ABSTRACT

Protease-activated receptor 2 (PAR2), a G protein-coupled receptor for trypsin, contributes to growth, anti-apoptosis, and migration in lung cancer. Given that PAR2 activation in airway epithelial cells compromises the airway epithelium barrier by disruption of E-cadherin adhesion, PAR2 may be involved in epithelial-mesenchymal transition (EMT) in lung adenocarcinoma cells. Although PAR2 is known to promote the migration of lung cancer cells, the detailed mechanism of this event is still not clear. Here, we found that PAR2 is highly expressed in several lung adenocarcinoma cell lines. In two lung adenocarcinoma cell lines, CL1-5 and H1299 cells, activation of PAR2 induces migration and Slug-mediated EMT. The underlying mechanisms involved in PAR2-induced migration and EMT in CL1-5 cells were further investigated. We showed that PAR2-induced migration of CL1-5 cells is mediated by the Src/p38 mitogen-activated protein kinase (p38 MAPK) signaling pathway. β-arrestin 1, not G protein, is involved in this PAR2-mediated Src/p38 MAPK signaling pathway. PAR2-induced EMT in CL1-5 cells is dependent on the activation of extracellular-signal-regulated kinase 2 (ERK2). The activation of ERK2 further mediates Slug stabilization through suppressing the activity of glycogen synthase kinase 3β. In addition, a poor prognosis was observed in lung adenocarcinoma patients with a high expression of PAR2. Thus, PAR2 regulates migration through β-arrestin 1-dependent activation of p38 MAPK and EMT through ERK2-mediated stabilization of Slug in lung adenocarcinoma cells. Our finding also suggests that PAR2 might serve as a therapeutic target for metastatic lung adenocarcinoma and a potential biomarker for predicting the prognosis of lung adenocarcinoma.

1. Introduction

Lung cancer is the most frequently diagnosed cancer and the most common cause of cancer-related death worldwide [1]. The survival rate is poor for patients with metastatic lung cancer. Within the tumor microenvironment, both cancer cells and neighboring non-cancer cells secrete proteases to facilitate cancer metastasis [2]. Serine proteases, a class of proteases, are involved in cancer metastasis by activating

Abbreviations: ABTS, 2,2′-azino-bis-3-ethylbenzthiazoline-6-sulfonic acid; 2f-LI, 2-furoyl-LIGRLO-NH_2; 18S rRNA, 18S ribosomal RNA; BMP-2, bone morphogenetic protein-2; BSA, bovine serum albumin; C, circularity; CCL4, chemokine C−C motif chemokine ligand 4; CCLE, cancer cell line encyclopedia; Cdc42, cell division cycle 42; cDNAs, complementary DNAs; C_T, threshold cycle; DMSO, dimethyl sulfoxide; D-PBS, Dulbecco's phosphate-buffered saline; EGFR, epidermal growth factor receptor; EMT, epithelial-mesenchymal transition; ERK, extracellular-signal-regulated kinase; FBS, fetal bovine serum; GP-2A, GP antagonist-2A; GPCR, G protein-coupled receptor; GSK3β, glycogen synthase kinase 3β; HPRT1, hypoxanthine phosphoribosyltransferase 1; IPTG, isopropyl β-Dthiogalactopyranoside; JNK, c-Jun N-terminal kinase; KLK6, kallikrein-related peptidase 6; MAPK, mitogen-activated protein kinase; MAPKAPK2, mitogen-activated protein kinase-activated protein kinase 2; MEK, MAPK kinase; MET, mesenchymal-epithelial transition; MMPs, matrix metalloproteases; NF-κB, nuclear factor kappa-light-chain-enhancer of activated B cells; Notch-1, notch homolog-1; OD, optical density; OS, overall survival; p115-RGS, RGS domain of p115-Rho guanine nucleotide exchange factor; P2pal-18S, palmitate-RSSAMDENSEKKRKSAIK-NH_2; PAR2, protease-activated receptor 2; PI3K, phosphatidylinositol 3-kinase; PKC, protein kinase C; PMSF, phenylmethylsulfonyl fluoride; PTX, pertussis toxin; PVDF, polyvinylidene difluoride; qRT-PCR, quantitative real-time polymerase chain reaction; RFS, recurrent free survival; RGS, regulator of G-protein signaling; RIPA, radioimmunoprecipitation assay lysis; RPMI-1640, Roswell Park Memorial Institute-1640; RT-PCR, reverse transcription-polymerase chain reaction; SD, standard deviation; shRNAs, short hairpin RNAs; siRNAs, small interfering RNAs; TBST, tris-buffered saline with 0.1% tween-20; TCGA, The Cancer Genome Atlas; TFs, transcription factors; TGF-β1, transforming growth factor-β1; Wnt, wingless/int-1 class

* Corresponding author at: Institute of Molecular and Cellular Biology, National Tsing Hua University, 101, Sec 2, Kuang-Fu Road, Hsinchu 30013, Taiwan, ROC.
E-mail addresses: ytchou@life.nthu.edu.tw (Y.-T. Chou), hwfu@life.nthu.edu.tw (H.-W. Fu).

https://doi.org/10.1016/j.bbamcr.2018.10.011
Received 18 December 2017; Received in revised form 31 August 2018; Accepted 11 October 2018
Available online 13 October 2018

specific surface proteins or receptors. Kallikrein-related peptidase 6 (KLK6) and trypsin, two serine proteases which activate protease-activated receptor 2 (PAR2), are associated with the proliferation and metastasis of cancer cells and are overexpressed in lung adenocarcinoma cells [3–5]. Hence, PAR2 may be involved in the development of lung cancer mediated by the serine proteases.

PAR2 belongs to a four-member family of G protein-coupled receptors (GPCRs) which are activated by serine proteases [6]. In this four-member family, PAR1, PAR3, and PAR4 are preferentially activated by thrombin, whereas PAR2 is mainly activated by trypsin [6]. The activation of PAR2 occurs through a proteolytic cleavage by serine proteases at the specific sites within the extracellular N-terminal domain of PAR2 [7]. Trypsin cleaves human PAR2 at the canonical site, $R^{36}\downarrow S^{37}$, to reveal the new N-terminal sequence starting with SLIGKV [7]. The newly exposed amino terminus acts as a tethered ligand to trigger transmembrane signaling mediated by G proteins and β-arrestins [8–10]. The synthetic agonist peptide, SLIGKV-NH_2, mimicking the tethered ligand of PAR2 can directly induce receptor activation [7]. Other serine proteases, such as tryptase, coagulation factors VIIa/tissue factor complex, acrosin, granzyme A, membrane-type serine protease 1, transmembrane protease serine 2, and KLK2, 4, 5, 6, and 14, and the cysteine protease gingipain-R from *Porphyromonas gingivalis* also activate PAR2 through the cleavage of this canonical site [6,11–20]. The cleavage of PAR2 at the non-canonical cleavage sites also induce the receptor activation. The cysteine protease cathepsin S is known to cleave PAR2 at the non-canonical cleavage sites, $G^{41}\downarrow K^{42}$ and $E^{56}\downarrow T^{57}$, to induce PAR2 signaling [21,22]. In addition, some serine proteases cleave PAR2 at the non-canonical sites to disarm the activity of the receptor by preventing the receptor activation through the canonical mechanism. These serine proteases include elastase, which cleaves PAR2 at $S^{67}\downarrow V^{68}$, cathepsin G, which cleaves PAR2 at $F^{64}\downarrow S^{65}$, and proteinase 3, which cleaves PAR2 at $V^{61}\downarrow D^{62}$ [23]. It has been reported that matrix metalloproteases (MMPs), such as MMP-1, -3, -8, -9, and -13, are activated by trypsin [24,25]. Among these MMPs, MMP-1 was shown to activate PAR2 in cancer cells [26]. However, it is not clear whether MMP1 activates PAR2 by a direct cleavage. Although PAR2 is mainly activated by trypsin but not by thrombin, it has been shown that high concentrations of thrombin can directly activate PAR2 through the cleavage of PAR2 at the canonical site [27]. Such high level of active thrombin can be generated in the patients with blunt trauma or cancer [28,29]. Thus, thrombin may also active PAR2 at sites of acute injury or in the tumor microenvironment.

PAR2 not only mediates a variety of physiological responses but also participates in cancer progression [6]. Overexpression of PAR2 has been found in various cancers, such as ovarian, uterine cervix, and lung [30–32]. This receptor also promotes proliferation, migration, and metastasis in these cancers [30,32–35]. Thus, overexpression or altered activation of PAR2 in cancer cells may contribute to cancer progression. It has been reported that PAR2 promotes proliferation of lung adenocarcinoma A549 cells through an epidermal growth factor receptor (EGFR)-dependent signaling pathway and induces migration of these cells by suppressing the expression of microRNA-125b [33–35]. However, the mechanism by which PAR2 regulates the proliferation and migration of lung cancer cells is largely unknown.

Initiation of cancer metastasis requires cell invasion which is promoted by epithelial-mesenchymal transition (EMT). The transition of epithelial cells to mesenchymal cells is accomplished by the loss of cell-cell adhesion and cell polarity and the acquisition of the ability to migrate and invade [36]. Generally, adhesion of cells to other cells is mediated by various adhesion molecules, such as E-cadherin. Suppression of E-cadherin expression is considered to be a fundamental event during the process of EMT. The expression of E-cadherin is mainly regulated by EMT-inducing transcription factors (TFs), which include the members of the Snail superfamily of zinc finger proteins, the Twist family of bHLH proteins, and the ZEB family of zinc finger *E*-box-binding homeobox proteins [36]. Among them, Snail1, Slug, ZEB1, and Twist1 are able to suppress the expression of E-cadherin to induce EMT in lung cancer cells [37–40]. In these cells, EMT can be triggered by various extracellular factors, such as TGF-β1, bone morphogenetic protein-2 (BMP-2), and thrombin [37,41–44]. Thrombin can activate PAR1, PAR3, and PAR4 to induce EMT in lung cancer cells [42–44]. However, it is not clear whether PAR2 is able to induce EMT in lung cancer cells. It has been reported that PAR2 activation induces the permeability of lung vessel in mice [45]. Activation of PAR2 also disrupts E-cadherin adhesion to increase the paracellular permeability of airway epithelium [46]. These findings suggest that PAR2 induces phenotypic changes of airway epithelial cells by interruption of E-cadherin binding. Loss of E-cadherin adhesion is a critical hallmark of EMT and is associated with tumor metastasis [36]. The evidence that PAR2 activation disrupts E-cadherin-mediated binding of lung epithelial cells supports the idea that PAR2 plays a role in the induction of EMT in lung cancer cells.

Although it has been previously reported that PAR2 induces migration of lung adenocarcinoma cells, the mechanism underlying this event is still unclear. It is also not known whether PAR2 promotes EMT in lung adenocarcinoma cells. In the present study, we first investigated how PAR2 regulates migration of lung adenocarcinoma cells and further examined whether G proteins or β-arrestins are involved in PAR2-mediated cell migration in lung adenocarcinoma cells. Then, we explored whether PAR2 induces EMT in lung adenocarcinoma cells and characterized the signaling pathways involved in this process. Finally, we examined whether the expression of PAR2 is correlated with the survival rate of patients with lung adenocarcinoma by analyzing The Cancer Genome Atlas (TCGA) database.

2. Materials and methods

2.1. Cell culture

The human lung adenocarcinoma cell lines, CL1-0 and CL1-5 [47], were gifts from Dr. Cheng-Wen Wu. H1299 lung adenocarcinoma cells were obtained from the American Type Culture Collection (Manassas, VA, USA). All lung adenocarcinoma cells were cultured in RPMI-1640 medium (Thermo Fisher Scientific, Rockford, IL, USA) supplemented with 10% characterized fetal bovine serum (FBS) (Hyclone, Piscataway, NJ, USA), 100 units/ml penicillin, and 100 μg/ml streptomycin (Thermo Fisher Scientific) in a humidified incubator with 5% CO_2 at 37 °C.

2.2. Plasmids and small interfering RNAs

The pcDNA3.1 (+) mammalian expression vector containing complementary DNA (cDNA) encoding wild-type human Slug [48], the pcDNA3 mammalian expression vector containing cDNA encoding HA-tagged constitutively active mitogen-activated protein kinase (MAPK) kinase 2 (MEK2) [49], the pCMV5-myc mammalian expression vector containing cDNA encoding the regulator of G protein signaling (RGS) domain of p115-Rho guanine nucleotide exchange factor (p115-RGS) [50], the PSP65SRα mammalian expression vector containing cDNA encoding a kinase-dead mutant of Src (SrcK298A) or a kinase-dead and autophosphorylation-defective mutant of Src (SrcK298AY419F) [51], and the pOP13 mammalian expression vector containing cDNA encoding an inducible dominant-negative mutant of p38 MAPK (T180AG181GY182F) [52], were used in the transfection experiments. The SureSilencing short hairpin RNA (shRNA) plasmids targeting human PAR2 and the scrambled shRNA plasmid were purchased from Qiagen (Valencia, CA, USA). The sequences of shRNA targeting PAR2 are 5′-TGGGAGACATGTTCAATTACT-3′ (shPAR2 sequence 1, shPAR2 #1) and 5′-CCATGTCTATGCCCTGTACAT-3′ (shPAR2 sequence 4, shPAR2 #4), and the sequence of scrambled shRNA is 5′-ACACTAAG TACGTCGTATTAC-3′. The small interfering RNAs (siRNAs) targeting human β-arrestin 1, β-arrestin 2, ERK1, and ERK2 were purchased from

Dharmacon (Lafayette, CO, USA). The sequences of siRNA targeting β-arrestin 1 and β-arrestin 2 are 5′-AAAGCCUUCUGCGCGGAGAAU-3′ and 5′-AAGGACCGCAAAGUGUUUGUG-3′ [53], respectively. The sequences of siRNA targeting ERK1 and ERK2 are 5′-GCCAUGAGAGAU GUCUACA-3′ and 5′-GAGGAUUGAAGUAGAACAG-3′, respectively. The sequence of scrambled siRNA is 5′-AAUUCUCCGAACGUGUCACGU-3′ [53].

2.3. Transient transfection of CL1-5 cells with shRNAs, siRNAs, and cDNAs

Transfection of shRNAs, siRNAs, and cDNAs was carried out using lipofectamine 2000 (Thermo Fisher Scientific) according to the manufacturer's instructions. CL1-5 cells were seeded at a density of 8×10^5 cells per 60-mm culture dish at 37 °C for 24 h and then transfected with 8 μg of shRNAs, 200 nM siRNAs, or 8 μg of cDNAs. For studying whether overexpression of Slug reverses the mesenchymal-epithelial transition (MET) induced by PAR2 knockdown, cells were co-transfected with 6 μg of shRNA targeting PAR2 and 2 μg of the plasmid expressing Slug. After 48 h of transfection, the cells were subjected to the subsequent analysis.

2.4. Generation of CL1-0 cells stably expressing PAR2

CL1-0 cells were seeded at a density of 5×10^5 cells per 60-mm culture dish at 37 °C for 24 h and then transfected with 2 μg of the plasmid encoding a hygromycin resistance gene together with 2 μg of the pBJ mammalian expression vector containing the cDNA encoding Flag-tagged PAR2 [12] or 2 μg of the pBJ vector as a control. Transfected cells were selected and grown under RPMI-1640 complete medium containing 1000 μg/ml hygromycin B (Thermo Fisher Scientific) for one month. Every three days, cells were changed to the fresh medium containing hygromycin B within this one-month period. The cell colonies were individually transferred into wells of 24-well plates and grown until reaching 90% confluency. These colonies were first screened for the expression of PAR2 on the cell surface by using a cell surface ELISA. Then, the expression of PAR2 in these colonies was confirmed by Western blotting using the anti-Flag M1 monoclonal antibody (Sigma, St Louis, MO, USA).

2.5. Cell surface ELISA

CL1-0 and CL1-5 cells were seeded in a 24-well plate at a density of 8×10^4 cells per well. After 24 h of cell attachment, the cells were washed with Dulbecco's phosphate-buffered saline (D-PBS) and then fixed with 4% paraformaldehyde in D-PBS at 4 °C for 10 min. After being washed with ice-cold the wash medium, which composed of serum-free RPMI-1640 medium supplemented with 20 mM HEPES, pH 7.4 and 1 mg/ml bovine serum albumin (BSA), for once, the cells were incubated with one of the three anti-PAR2 antibodies and its corresponding IgG antibody or serum listed in Supplementary Table S1 at a concentration of 2 μg/ml in the wash medium at room temperature for 1 h. The cells were then washed with the wash medium once and incubated with the species-appropriate horseradish peroxidase-conjugated secondary antibody (Jackson ImmunoResearch, West Grove, PA, USA) at a dilution of 1:5000 in the wash medium at room temperature for 1 h. After the cells were washed twice with the wash medium and once with D-PBS, the amount of bound secondary antibody was detected by incubating the cells with 250 μl of 1-Step ABTS (2,2′-azino-bis-3-ethylbenzthiazoline-6-sulfonic acid, Thermo Fisher Scientific) at room temperature for 30 min. Aliquots of 200 μl were transferred to the wells of a 96-well plate. The optical densities (OD) of these aliquots were determined at 415 nm using iMARK Microplate Absorbance Reader (Bio-Rad Laboratory, Hercules, CA, USA). The cells were washed once with D-PBS and then were treated with 0.05% trypsin/EDTA (Thermo Fisher Scientific) at room temperature for 3 min. The detached cells were counted with a hemocytometer. The OD value of each cell was calculated by dividing the OD value measure from each well by the number of the cells counted in the same well. The amounts of cell surface PAR2 expressed in each cell were obtained by subtracting the OD value of each cell incubated with the IgG or serum from the OD value of each cell incubated with the anti-PAR2 antibodies.

2.6. Treatment with the PAR2 agonist and inhibitors

The peptide SLIGKV-NH_2, a PAR2 agonist, and palmitate-RSSAM-DENSEKKRKSAIK-NH_2 (P2pal-18S), a PAR2 pepducin antagonist, were synthesized by Angene Biotech (Taipei, Taiwan) and used for treating cells at a concentration of 100 and 10 μM, respectively. The peptide 2-furoyl-LIGRLO-NH_2 (2f-LI), a PAR2 agonist, and VKGILS-NH_2 (VKGILS), a control peptide for SLIGKV-NH_2, were purchased from Tocris Bioscience (Bristol, UK) and used for treating cells at a concentration of 1 and 100 μM, respectively. GB83 (Axon Medchem, Groningen, The Netherlands), a PAR2 small molecule antagonist, was used for treating cells at a concentration of 50 μM unless specified. Isopropyl β-Dthiogalactopyranoside (IPTG) (Sigma) was used for treating cells at a concentration of 5 mM. GP antagonist-2A (GP-2A), an inhibitor of Gq, E-64, an inhibitor of cysteine proteases, and GM6001, a broad-spectrum inhibitor of MMPs, were purchased from Enzo Life Sciences (Farmingdale, USA) and used for treating cells at a concentration of 5, 10, and 5 μM, respectively. Pertussis toxin (PTX) (Merck, Billerica, MA, USA), a Gi inhibitor, was used for pretreating cells at a concentration of 0.1 μg/ml for 16 h. Dasatinib (Santa Cruz Biotechnology, Santa Cruz, CA, USA), a Src inhibitor, was used for pretreating cells at a concentration of 100 nM for 1 h unless specified. PD98059, a MEK1/2 inhibitor, and SB202190, a p38 MAPK inhibitor, were purchased from Adooq Bioscience (Irvine, CA, USA) and used for pretreating cells at a concentration of 15 and 20 μM, respectively, for 1 h unless specified. Phenylmethylsulfonyl fluoride (PMSF) (Roche, Basel, Switzerland), a serine protease inhibitor, was used for treating cells at a concentration of 1 mM. Tunicamycin (Sigma) at a concentration of 2 μg/ml was used for treating cells for 16 h to inhibit N-linked protein glycosylation. TWS119 (AbMole BioScience, Houston, TX, USA) at a concentration of 50 nM was used for treating cells for 18 h to inactivate glycogen synthase kinase 3β (GSK3β).

2.7. Migration and invasion assay

Migration assay was performed using 8 μm pore FluoroBlok transwell inserts (BD Biosciences, San Diego, CA, USA) coated with 100 μg/ml gelatin (Sigma) as described in the manufacturer's protocol. Cells were serum starved in serum-free RPMI-1640 medium at 37 °C for 24 h and then trypsinized and suspended in serum-free RPMI-1640 medium. The cells were treated with the PAR2 agonist or inhibitors and then seeded at a density of 1.4×10^5 cells/ml in the upper chamber of the transwell insert. RPMI-1640 medium supplemented with 10% FBS, which was used as chemoattractant, was added to the lower transwell chamber. After 6 h of incubation, the migrated cells on the lower surface of the transwell insert were stained with 50 μg/ml propidium iodide (Thermo Fisher Scientific) and visualized at a magnification of 200× using an Axiovert 200 inverted fluorescence microscope (Zeiss, Germany). The migrated cells were counted from five randomly picked fields using Image J software (NIH, Maryland, USA) and the average of the numbers of migrated cells was calculated using Excel 2010 (Microsoft, Roselle, IL, USA). Invasion assay was performed in the same manner as the migration assay except that cells were seeded at a density of 7×10^4 cells/ml in the upper chamber of the transwell insert coated with 1 mg/ml matrigel (BD Biosciences) with incubation for 24 h. These two assays were both performed in duplicate.

2.8. Analysis of the morphology changes of CL1-5 cells during the process of MET

Photomicrographs were captured at a magnification of 200× using an Axiovert 200 inverted fluorescence microscope (Zeiss) equipped with AxioCam HRm CCD camera (Zeiss) controlled by Axio Vision 4 software (Zeiss). Cells that displayed an elongated shape were defined as mesenchymal-like cells, whereas cells that displayed a round shape were defined as epithelial-like cells. Cell circularity (C) was analyzed by using Image J software (NIH) and calculated by using the formula $C = 4\pi(area/perimeter^2)$. The circularity value of 1 indicates a perfect round shape, while the circularity value of 0 indicates an elongated shape. A cell is considered to have a round shape or an elongated shape when its circularity value is higher or lower than 0.6, respectively. The cell circularity was analyzed for at least 1000 cells in each experimental group. The percentage of cells with round or elongated shapes in each group was analyzed by Excel 2010 (Microsoft).

2.9. RNA extraction, reverse transcription-polymerase chain reaction, and quantitative real-time polymerase chain reaction

RNA extraction and reverse transcription-polymerase chain reaction (RT-PCR) were carried out as previously described [54], except that NucleoZOL (MACHEREY-NAGEL, Düren, Germany) was used to extract total RNA from cells and that the primers, annealing temperatures, and PCR cycle number listed in Supplementary Table S2 were used for PCR amplification. For quantitative real-time PCR (qRT-PCR), the PCR was carried out with 50 ng of the cDNA product, 2 μM primer pairs for the gene of interest, and 2× SYBR green (Applied Biosystems, Foster City, CA, USA) by using StepOnePlus real-time PCR system (Applied Biosystems) programmed with the following amplification conditions: 1 cycle of 95 °C for 6 min, followed by 40 cycles of 95 °C for 45 s, 55 °C for 30 s, and 72 °C for 30 s, and a final cycle of 72 °C for 5 min. The sequences of the primer pairs targeting PAR2, Slug, and hypoxanthine phosphoribosyltransferase 1 (HPRT1) are listed in Supplementary Table S2. The threshold cycle (C_T) of PCR amplification was obtained by the StepOne software (Applied Biosystems). Then, the comparative threshold cycle method ($2^{-\Delta\Delta CT}$) was used to calculate the relative expression levels of genes between different experimental groups.

2.10. Cell growth assay

Cell growth was assayed by using the alamar blue assay (Thermo Fisher Scientific), according to the manufacturer's instructions. Briefly, CL1-0 and CL1-5 cells were seeded in a 96-well plate at a density of 1×10^4 and 5×10^4 cells per well, respectively. After 24 h of cell attachment, cells were serum starved with serum-free RPMI-1640 medium at 37 °C for 24 h. Then, serum-starved cells were treated with 100 μM VKGILS-NH_2, 100 μM SLIGKV-NH_2, 1 μM 2f-LI, 50 μM GB83, 10 μM P2pal-18S, 0.17% (v/v) dimethyl sulfoxide (DMSO) (Sigma), or 10% FBS, as a positive control, at 37 °C for 6, 24, 48, 72, and 96 h. For determination of the viable cells, alamar blue was added to the culture medium at a final concentration of 10% (v/v) for 1 h prior to measurement of the fluorescence of each well at the indicated time. The emission of fluorescence at 595 nm was measured with excitation at 530 nm by using a Victor 3 microplate reader (Perkin Elmer, Norwalk, CT, USA). The assay was performed in triplicate.

2.11. Western blotting

Cells were harvested in a modified radioimmunoprecipitation assay lysis (RIPA) buffer containing 10 mM Tris-HCl, pH 7.4, 150 mM NaCl, 0.05% SDS, 1% NP-40, 0.5 mM EDTA, with the addition of 0.2 mM PMSF, 1 μg/ml aprotinin, 4 μM leupeptin, 1 mM Na_3VO_4, 1 μM pepstatin A, and 1 mM NaF. The cell suspension was sonicated thirty times with 50% amplitude and 0.5 cycle on ice using an UP50H ultrasonic processor (Dr. Hielscher, Berlin, Germany). The insoluble protein was removed by centrifugation at 12,000 × *g* at 4 °C for 15 min. Protein concentrations were determined by the Bradford method (Bio-Rad protein Assay, Bio-Rad Laboratory). Equal amounts of cell lysates were subjected to SDS-PAGE with gels containing 7.5%, 10%, or 15% acrylamide according to the molecular masses of the proteins of interest. In this study, 7.5% and 15% gels were used to separate the proteins with molecular masses above 100 kDa and below 30 kDa, respectively. A 10% gel was used to separate the proteins with molecular masses between 40 and 100 kDa. An excelband 3-color pre-stained protein marker (SMOBiO, Hsinchu, Taiwan) was used as a molecular weight standard. After electrophoresis, proteins were transferred onto a polyvinylidene difluoride (PVDF) membrane (Millipore, Bedford, MA, USA). The membrane was blocked with 5% BSA in Tris-buffered saline (TBS) with 0.1% Tween-20 (TBST) containing 50 mM Tris-HCl, pH 7.4 and 15 mM NaCl at room temperature for 1 h. Then, the membrane was probed with the primary antibody which was prepared in TBST containing 5% BSA at 4 °C overnight. Detailed descriptions and working dilutions of the primary antibodies are listed in Supplementary Table S1. The antibody-probed membrane was washed with TBST containing 5% fat-free milk (5% TBST/milk) three times for 10 min and then probed with the species-appropriate horseradish peroxidase-conjugated secondary antibody (Jackson ImmunoResearch), which were prepared in 5% TBST/milk at a dilution of 1:5000, at room temperature for 1 h. After the membrane was washed three times for 10 min by TBS, chemiluminescent detection was performed using Immobilon Western Chemiluminescent HRP Substrate (Millipore). The bands were imaged by LAS-3000 imaging system (Fujifilm, Tokyo, Japan) and quantified using densitometry by MultiGauge software version 3.0 (Fujifilm).

2.12. The cancer cell line encyclopedia database analysis

The dataset of 967 cancer cell lines across 36 types of cancer from the Cancer Cell Line Encyclopedia (CCLE) database was obtained from the UCSC Cancer Browser website (https://genome-cancer.ucsc.edu/proj/site/hgHeatmap/). In this dataset, data of $\log_2$-transformed expression of PAR2 in these 967 cancer cell lines were downloaded. The data of the fold-change of PAR2 expression in the 56 lung adenocarcinoma cell lines were selected and shown in Supplementary Table S3 and created as a bar graph by Excel 2010 (Microsoft).

2.13. Survival analysis

The sources of gene expression profiling data of lung adenocarcinoma and the corresponding clinicopathological parameters were downloaded from TCGA (https://tcga-data.nci.nih.gov/docs/publications/luad_2014/). The median level of PAR2 expression was used as the cut-off point for survival correlation analysis.

2.14. Statistical analysis

Overall survival (OS) and recurrent free survival (RFS) were estimated by the Kaplan-Meier method and both survival curves were generated with Prism 5.0 (GraphPad Software Inc., San Diego, CA, USA). The differences of OS and RFS between the high and low gene expressing groups were compared by log-rank test. The correlation of the mRNA expression of PAR2 and the number of migrated lung adenocarcinoma cells was estimated by the Spearman's rank correlation coefficient analysis using Excel 2010 (Microsoft). Significance of the correlation coefficient was calculated by ANOVA. Statistical significance of all other data was analyzed by a Student's *t*-test using Excel 2010. All data are presented as mean ± SD. $P < 0.05$ is considered as statistically significant.

3. Results

3.1. PAR2 is overexpressed in CL1-5, a lung adenocarcinoma cell line with high invasion ability

To determine whether PAR2 is overexpressed in lung adenocarcinoma cells, we examined the expression level of PAR2 in lung adenocarcinoma cell lines using the CCLE database. In the total of 56 available lung adenocarcinoma cell lines examined, 75% of them were positive for PAR2 mRNA expression (Supplementary Fig. S1A). More than 71% of these PAR2-positive cell lines showed an increase of PAR2 mRNA expression of at least 2-fold (Supplementary Fig. S1A). As shown in the RT-PCR analysis depicted in Supplementary Fig. S1B, the mRNA expression of PAR2 was much higher in four lung adenocarcinoma cell lines, H1975, A549, H358, and H1299, than that in the normal bronchial epithelium cell line NL20. The mRNA expression of PAR2 was not detectable in the lung adenocarcinoma cell line H1437 (Supplementary Fig. S1B). The finding obtained by RT-PCR analysis for the cells listed in CCLE database is consistent with the result obtained from this database. Therefore, PAR2 overexpression is common in lung adenocarcinoma cells.

We further investigated the relationship between the expression level of PAR2 and the ability of migration and invasion in lung adenocarcinoma cells. In this experiment, two lung adenocarcinoma cells, CL1 cells, which are also designated as CL1-0 cells [47] and CL1-5 cells, a subline of CL1 cells [55], were used for studying the migration and invasion in response to PAR2 activation. The chosen of CL1-5 cells is because these cells were selected from CL1-0 cells based on their high invasiveness [55]. Consistent with the previous report [47,55], CL1-5 cells did show higher ability of migration and invasion as compared to CL1-0 cells (Supplementary Fig. S2). In addition, we found that CL1-5 cells expressed more PAR2 than CL1-0 cells at the mRNA level (Fig. 1A). We then examined whether CL1-5 cells expressed more cell-surface PAR2 than CL1-0 cells by using a cell surface ELISA with three commercially PAR2 antibodies, SAM11, D61D5, and N19. These three antibodies are against the amino acid residues located near the N-terminus of PAR2. Both SAM11 and D61D5 antibodies, not the N19 antibody, detected higher levels of PAR2 on the surface of CL1-5 cells than that of CL1-0 cells (Fig. 1B). In addition, the level of cell-surface PAR2 on CL1-5 cells detected by the D61D5 antibody was higher than that detected by the SAM11 antibody (Fig. 1B). These results indicate that both SAM11 and D61D5 antibodies are able to distinguish the differential expression of surface PAR2 between CL1-0 and CL1-5 cells. We also examined the protein expression of PAR2 in these two cells by Western blot analysis with the three PAR2 antibodies. In CL1-5 cells, an extra band at ~100 kDa was detected by the SAM11 antibody and the additional smear bands, ranging from ~140 to ~45 kD, were detected by the D61D5 antibody (Fig. 1C). However, a similar pattern of multiple bands ranging from ~140 to ~45 kD was detected in CL1-0 and CL1-5 cells by the N19 antibody (Fig. 1C). To further confirm that the extra band or the additional bands detected in CL1-5 cells by SAM11 or D61D5 antibodies are PAR2-specific, we examined whether these bands disappeared after knockdown of PAR2. As shown in Fig. 1D, the intensities of the extra band and the additional smear bands detected by SAM11 and D61D5 antibodies, respectively, were markedly reduced in CL1-5 cells transfected with the two independent PAR2-specific shRNAs. It has been previously reported that PAR2 migrated as the smear bands ranging from 100 to 55 kDa, which is greater than the predicted molecular mass of 44 kDa, due to differential glycosylation [56]. To determine whether the smear bands detected by the D61D5 antibody are the differentially glycosylated forms of PAR2, we treated CL1-0 and CL1-5 cells with tunicamycin, an inhibitor of N-linked glycosylation, to examine whether inhibition of N-linked glycosylation affects the pattern of protein bands detected by the D61D5 antibody. After treatment of CL1-5 cells with tunicamycin, intense protein bands ranging from ~37 to ~30 kDa were detected by the D61D5 antibody, whereas only very faint bands appeared in the range of ~140 to ~45 kD (Supplementary Fig. S3). Treatment of CL1-0 cells with tunicamycin did not change the pattern of protein bands (Supplementary Fig. S3). These results indicate that the additional smear bands detected by the D61D5 antibody in CL1-5 cells should be the differentially glycosylated forms of PAR2. The extra band detected by the SAM11 antibody in CL1-5 cells could also be one specific form of glycosylated PAR2. Although it has been reported that the N19 antibody is able to specifically detect endogenous PAR2 in the two prostate cancer cells, DU145 and PC3, by Western blot analysis [57], it is not clear whether the multiple bands detected by N19 in both CL1-0 and CL1-5 cells are PAR2-specific. The finding that CL1-5 cells express more PAR2 than CL1-0 cells as detected by SAM11 and D61D5 antibodies is consistent with the result obtained by qRT-PCR analysis. Thus, the level of PAR2 expression is correlated with the ability of migration and invasion in these two lung adenocarcinoma cells. Because the D61D5 antibody detected more cell-surface PAR2 and more various forms of glycosylated PAR2 expressed in CL1-5 cells as compared to the SAM11 antibody, the D61D5 antibody was chosen to detect the expression of PAR2 in CL1-0 and CL1-5 cells. Although the SAM11 antibody detected less surface-expressed PAR2 in CL1-5 cells than the D61D5 antibody, both antibodies are able to detect the differential expression of surface PAR2 in CL1-0 and CL1-5 cells. When the SAM11 or D61D5 antibodies are used for detecting PAR2 expression, cell surface ELISA could serve as an alternative approach to quantify the surface expression of PAR2 in different cell lines.

3.2. PAR2 mediates the migration and invasion of CL1-5 cells

To investigate whether the differential expression of PAR2 affects the migration and invasion of CL1-5 and CL1-0 cells, we first examined whether knockdown of PAR2 in CL1-5 cells affects their ability to migrate and invade. Knockdown of PAR2 by the two independent PAR2-specific shRNAs significantly reduced the migration and invasion in these two PAR2-silenced CL1-5 cells (Fig. 1E). We then examined whether overexpression of PAR2 promotes the migration of CL1-0 cells. The mRNA expression of PAR2 in the two CL1-0 clones stably overexpressing PAR2 was significantly higher than that in the vector control CL1-0 clone but lower than that in CL1-5 cells (Supplementary Fig. S4A). Also, the protein expression of PAR2 was markedly increased in the two CL1-0 clones stably overexpressing PAR2 (Fig. 1F). These two CL1-0 clones stably overexpressing PAR2 showed a 2.7-fold higher migration ability than the vector control CL1-0 clone (Fig. 1G). In addition, we examined the mRNA expression of PAR2 and the basal migration of another lung adenocarcinoma H1299 cells. The mRNA expression of PAR2 in H1299 cells was higher than that in CL1-0 cells but lower than that in CL1-5 cells (Supplementary Fig. S4A). The basal migration of H1299 cells was also higher than that of CL1-0 cells but lower than that of CL1-5 cells (Supplementary Fig. S4B). To determine whether the increase of PAR2 expression correlates with the increased migration of these lung adenocarcinoma cells, we further analyzed the correlation of mRNA expression of PAR2 and cell migration among CL1-0 cells, the vector control CL1-0 clone, the two CL1-0 clones stably overexpressing PAR2, CL1-5 cells, and H1299 cells. As shown in Supplementary Fig. S4C, there was a significant positive correlation between mRNA expression of PAR2 and cell migration among these six analyzed cell lines. Thus, the level of PAR2 expression is correlated with the degree of cell migration in lung adenocarcinoma cells.

We then treated CL1-0 and CL1-5 cells with the two PAR2 agonist peptides, SLIGKV-NH_2 and 2f-LI, to examine whether activation of PAR2 induces the migration of these two cells. Activation of PAR2 in CL1-0 cells by stimulation with SLIGKV-NH_2 or 2f-LI significantly increased the cell migration by 1.6- or 1.5-fold, respectively, while stimulation of CL1-5 cells with SLIGKV-NH_2 or 2f-LI led to a significant but only 1.3-fold increase in the cell migration (Fig. 1H). Treatment of CL1-0 and CL1-5 cells with the peptide VKGILS-NH_2, a reversed amino acid sequence control peptide for SLIGKV-NH_2, did not affect the

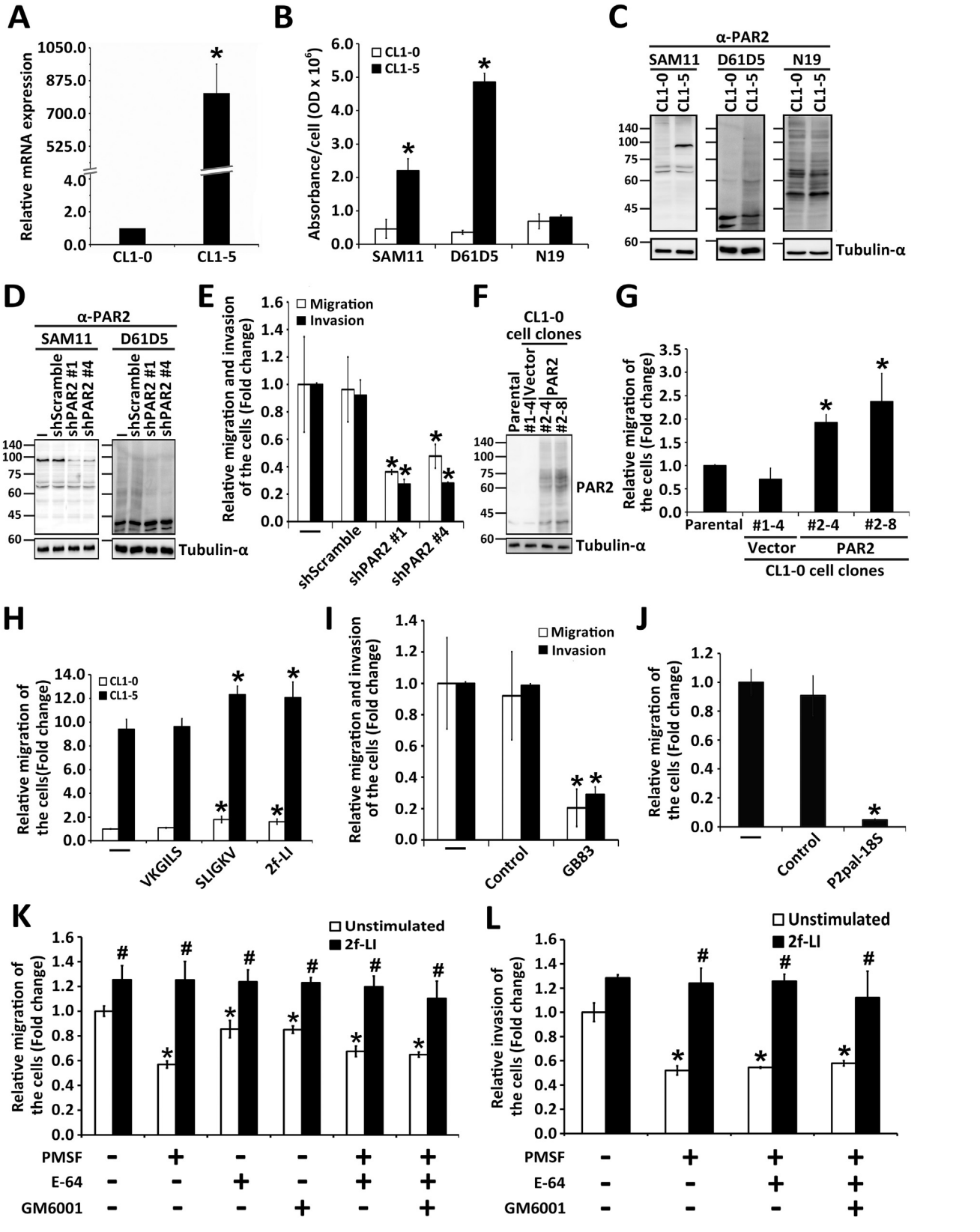

(caption on next page)

migration of both cells (Fig. 1H). These results indicate that the activity of PAR2 is involved in the migration of CL1-0 and CL1-5 cells. Because CL1-0 cells express much lower level of PAR2 than CL1-5 cells, we examined whether activation of PAR2 also induces the phosphorylation of extracellular-signal-regulated kinase 1/2 (ERK1/2) and p38 MAPK in these two cells. In CL1-0 cells, treatment with SLIGKV-NH_2 or 2f-LI induced the phosphorylation of ERK1 by 4.1- or 4.0-fold, respectively, and the phosphorylation of ERK2 by 3.7- or 3.8-fold, respectively

Fig. 1. PAR2 promotes the migration of CL1-0 and CL1-5 cells. (A) CL1-0 and CL1-5 cells were lysed and the mRNAs extracted from cell lysates were subjected to the reverse transcription reaction. The mRNA expression of PAR2 and HPRT1, as a loading control, was quantified by qRT-PCR. The mRNA expression of PAR2 was normalized to that of HPRT1. The quantitative values were expressed as relative mRNA levels by defining the amounts of PAR2 expression in CL1-0 cells as 1. Data are represented as the mean ± SD of three-independent experiments. (B) CL1-0 and CL1-5 cells were subjected to the cell surface ELISA to detect the cell surface expression of PAR2. Data are represented as the mean ± SD of three-independent experiments. (C) CL1-0 and CL1-5 cells were lysed and cell lysates were subjected to Western blotting for the detection of PAR2 and tubulin-α, as a loading control. Similar results were obtained in three-independent experiments. (D, E) CL1-5 cells were left untransfected (−) or transfected with two PAR2-specific shRNAs (shPAR2 #1 and #4) and scrambled shRNA (shScramble) for 48 h. The cells were subjected to Western blotting, migration, or invasion assays. (F, G) Parental CL1-0 cells, two CL1-0 clones stably expressing PAR2 (#2–4 and #2–8), or vector control CL1-0 clone (#1–4) were subjected to Western blotting or the migration assay. (H–J) Serum-starved CL1-5 cells were left untreated (−) or treated with 100 μM VKGILS-NH_2 (VKGILS) (H), 100 μM SLIGKV-NH_2 (SLIGKV) (H), 1 μM 2f-LI (H), 50 μM GB83 (I), 10 μM P2pal-18S (J), or DMSO (control) (I, J). The cells were then subjected to migration or invasion assays. (K, L) Serum-starved CL1-5 cells were treated with 1 mM PMSF, 10 μM E-64, 5 μM GM6001, 1 mM PMSF together with 10 μM E-64 plus/minus 5 μM GM6001, or DMSO plus isopropanol (−) and then left unstimulated or stimulated with 1 μM 2f-LI. The cells were then subjected to migration or invasion assays. (D, F) The cells were lysed and cell lysates were subjected to Western blotting for the detection of PAR2 and tubulin-α. The protein bands of PAR2 were detected by the D61D5 antibody unless specified. Tubulin-α was used as a loading control. Similar results were obtained in three-independent experiments. (E, G–L) The quantitative values were expressed as relative migration of the cells (E, G–K) or relative invasion of the cells (E, I, L) by defining the numbers of migrated or invaded cells of the untransfected group, the parental group, or the untreated group as 1. Data are represented as the mean ± SD of three-independent experiments. In A and B, $^{*}P < 0.05$ compared to CL1-0 cells. In E, $^{*}P < 0.05$ compared to cells transfected with scrambled shRNA. In G, $^{*}P < 0.05$ compared to vector control CL1-0 clone. In H, $^{*}P < 0.05$ compared to untreated cells. In I and J, $^{*}P < 0.05$ compared to DMSO-treated control cells. In K and L, $^{*}P < 0.05$ compared to the cells treated with DMSO plus isopropanol; $^{\#}P < 0.05$ compared to unstimulated cells in the same inhibitor-treated group.

(Supplementary Fig. S5). As to CL1-5 cells, treatment with SLIGKV-NH_2 or 2f-LI induced the phosphorylation of ERK1 by 1.7- or 1.9-fold, respectively, and the phosphorylation of ERK2 by 1.7-fold (Supplementary Fig. S5). Because of the higher basal activation of ERK1/2 in CL1-5 cells, the fold increase in the PAR2 agonist-induced phosphorylation of ERK1/2 is greater in CL1-0 cells. Treatment of CL1-0 cells with SLIGKV-NH_2 or 2f-LI induced the phosphorylation of p38 MAPK by 3.0- or 3.3-fold, respectively, while treatment of CL1-5 cells with SLIGKV-NH_2 or 2f-LI induced the phosphorylation of p38 MAPK by 2.9- or 2.8-fold, respectively (Supplementary Fig. S5). Interestingly, the ratios of fold increase in cell migration to fold increase in the phosphorylation of p38 MAPK induced by 2f-LI are similar in CL1-0 and CL1-5 cells. When CL1-0 and CL1-5 cells were treated with the negative control peptide, VKGILS-NH_2, the levels of phosphorylation of ERK1/2 and p38 MAPK were not changed in both cells (Supplementary Fig. S5). Thus, specific activation of PAR2 by its peptide agonists induces the phosphorylation of ERK1/2 and p38 MAPK in CL1-0 and CL1-5 cells. These findings also support the idea that PAR2 is functional in both CL1-0 and CL1-5 cells even though the expression level of PAR2 in CL1-0 cells is low.

To further examine whether inactivation of PAR2 suppresses the migration of CL1-5 cells, we treated this cell with a PAR2 small molecule antagonist, GB83, and a PAR2 pepducin antagonist, P2pal-18S, to inactivate PAR2. Treatment with 50 μM of GB83 significantly suppressed the basal migration and invasion of CL1-5 cells by 70% (Fig. 1I), while treatment with 10 μM of P2pal-18S almost completely suppressed the basal migration of CL1-5 cells (Fig. 1J). Thus, P2pal-18S is more potent than GB83 in inhibition of the basal migration of CL1-5 cells. These results also reveal that constitutive activation of PAR2 may contribute to the basal migration and invasion of CL1-5 cells. It is possible that the constitutive activation of PAR2 in CL1-5 cells is induced by the serine proteases, cysteine proteases, or MMPs expressed and/or secreted by this cells. To test this possibility, we treated CL1-5 cells with PMSF, an inhibitor of serine proteases, E-64, an inhibitor of cysteine proteases, and GM6001, a broad-spectrum inhibitor of MMPs, alone or in combination to examine their effects on cell migration and invasion. Treatment with PMSF significantly suppressed the basal migration of CL1-5 cells by 43% (Fig. 1K). Treatment with E-64 or GM6001 led to a significant but only 15% decrease in the migration of CL1-5 cells (Fig. 1K). However, treatment of CL1-5 cells with PMSF together with E-64 plus/minus GM6001 had no addictive effect on the inhibition of cell migration (Fig. 1K). The inhibitory effects of PMSF together with E-64 plus/minus GM6001 on the basal level of cell migration were similar to that of PMSF alone (Fig. 1K). In addition, treatment of CL1-5 cells with these three inhibitors did not significantly affect the cell viability (Supplementary Fig. S6A). In terms of invasion, PMSF treatment significantly suppressed the basal invasion of CL1-5 cells by 48% (Fig. 1L). Consistent with the result obtained from the migration assay, treatment of CL1-5 cells with PMSF together with E-64 plus/minus GM6001 had no addictive effect on the cell invasion (Fig. 1L). These results indicate that serine proteases, cysteine proteases, and MMPs secreted by CL1-5 cells all partially contribute the basal migration and invasion. Next, we evaluated whether PAR2 is responsible for the migration and invasion of CL1-5 cells induced by serine proteases, cysteine proteases, and MMPs secreted from this cell. In CL1-5 cells treated with PMSF alone or together with E-64 plus/minus GM6001, activation of PAR2 by 2f-LI, recovered the ability of these cells to migrate and invade to a similar level as that of the 2f-LI-treated control cells (Fig. 1K, L). Taken together, these results indicate that the elevated basal migration and invasion of CL1-5 cells resulted from the constitutive activation of PAR2 mediated by the serine proteases, cysteine proteases, and MMPs secreted by these cells.

To rule out that the migration induced by PAR2 is cell-type specific, we treated another lung adenocarcinoma H1299 cells, with the two PAR2 agonists, SLIGKV-NH_2 and 2f-LI, and the two PAR2 antagonists, GB83 and P2pal-18S, to examine their effects on cell migration. In H1299 cells, PAR2 was detected as multiple bands ranging from ~140 to ~45 kDa by the D61D5 antibody (Supplementary Fig. S7A). Stimulation of H1299 cells with SLIGKV-NH_2 or 2f-LI induced a 1.9-fold increase in cell migration (Supplementary Fig. S7B). Treatment of this cell with the negative control peptide, VKGILS-NH_2, did not affect the cell migration (Supplementary Fig. S7B). Inactivation of PAR2 in H1299 cells with GB83 or P2pal-18S reduced the cell migration by 20% or 77%, respectively (Supplementary Fig. S7C, D). These results indicate that PAR2 is involved in the migration of H1299 cells. Therefore, the activity of PAR2 is essential for regulating the migration of lung adenocarcinoma cells.

We also investigated whether activation of PAR2 affects the growth of CL1-5 and CL1-0 cells. A similar 4-day growth curve was observed in both of these cells stimulated with SLIGKV-NH_2 or 2f-LI or treated with the negative control peptide, VKGILS-NH_2 and the respective unstimulated cells (Supplementary Fig. S8A). This result indicates that PAR2 activation does not induce the growth of these two cells. Since PAR2 is constitutively activated in CL1-5 cells, we treated the cells with increasing concentrations of GB83 to examine whether inactivation of PAR2 inhibits the growth of CL1-5 cells. Treatment of GB83 at a concentration up to 50 μM did not affect the cell growth (Supplementary Fig. S8B). We then treated the cells with the PAR2 antagonist, P2pal-18S, to examine its effect on the growth of CL1-5 cells. Again, there is no difference in the growth of CL1-5 cells treated with P2pal-18S or DMSO (Supplementary Fig. S8C). These results indicate that PAR2 activity does not contribute to the growth of CL1-5 cells. Therefore, PAR2 plays an important role for the migration but not the growth of CL1-5

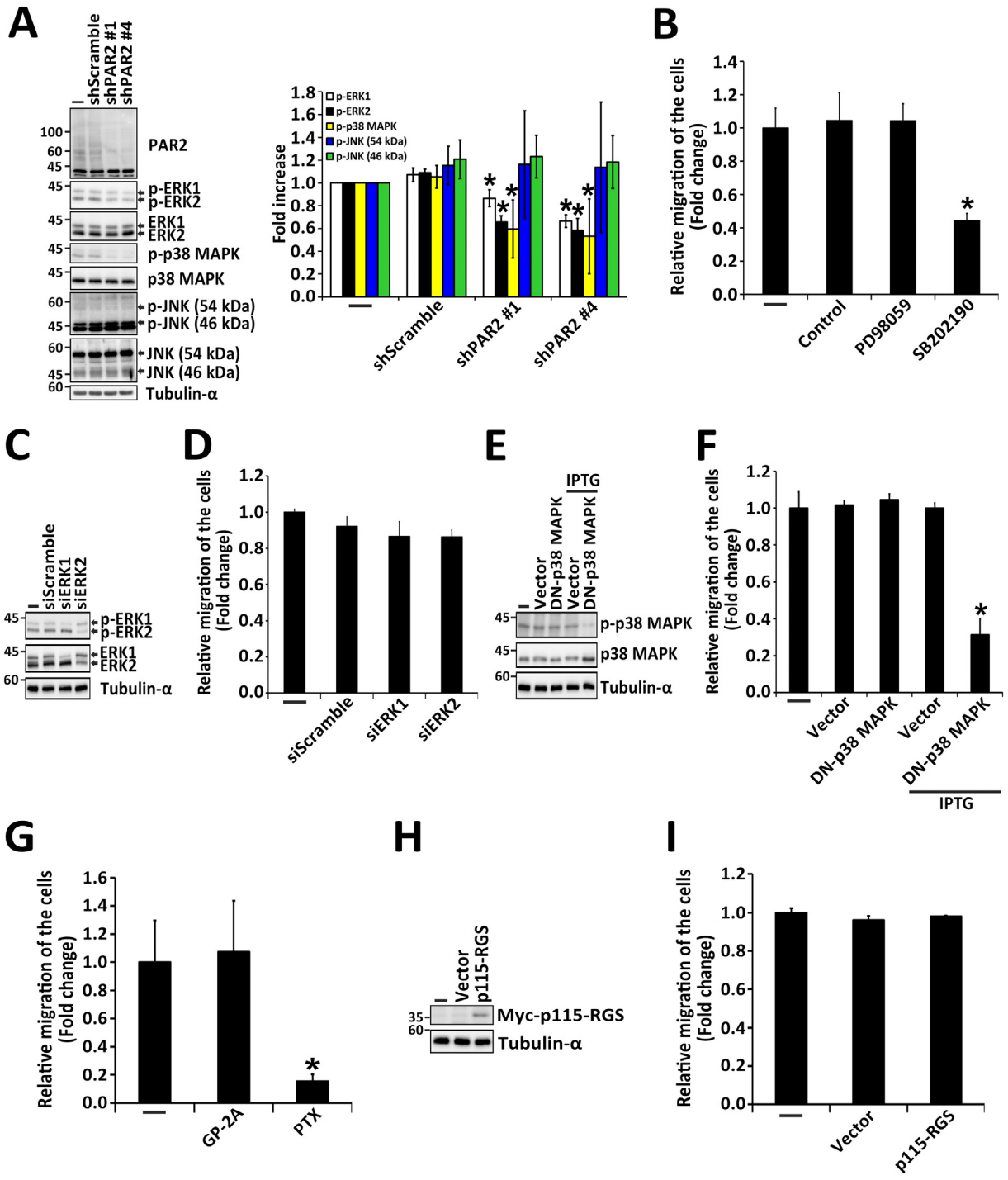

Fig. 2. p38 MAPK and Gi regulate PAR2-induced migration of CL1-5 cells. (A) CL1-5 cells were left untransfected (−) or transfected with two PAR2-specific shRNAs (shPAR2 #1 and #4) and scrambled shRNA (shScramble) for 48 h. (B) Serum-starved CL1-5 cells were left untreated (−) or treated with 15 μM PD98059, 20 μM SB202190, or DMSO (control). (C, D) CL1-5 cells were left untransfected (−) or transfected with 200 nM siRNAs specific to ERK1 and ERK2 or 200 nM scrambled siRNA (siScramble) for 48 h. (E, F) CL1-5 cells were left untransfected (−) or transfected with the plasmid encoding an inducible dominant-negative mutant of p38 MAPK (DN-p38 MAPK) or the control vector. After 24 h of transfection, these cells were left untreated or treated with 5 mM IPTG for 48 h. (G) Serum-starved CL1-5 cells were left untreated (−), treated with 5 μM GP-2A, or pretreated with 0.1 μg/ml PTX for 16 h. (H, I) CL1-5 cells were left untransfected (−) or transfected with the plasmid encoding myc-tagged p115-RGS or the control vector for 48 h. (A, C, E, H) The cells were then lysed and cell lysates were subjected to Western blotting for the detection of the indicated phospho-MAPKs and total MAPKs, PAR2, myc-p115-RGS, and tubulin-α. The protein bands of PAR2 were detected by the D61D5 antibody. The total MAPKs and tubulin-α were used as loading controls. Similar results were obtained in three-independent experiments. In A, the quantitative results were expressed as fold increase by defining the amounts of phosphorylated kinases in untransfected cells as 1. Data are represented as the mean ± SD of three-independent experiments. In C, the quantitative results of phospho-ERK1/2 and ERK1/2 in ERK1- and ERK2-silenced cells are shown in Fig. 7B. In E, the quantitative results of phospho-p38 MAPK and p38 MAPK in DN-p38 MAPK-expressed cells are shown in Fig. 6F. (B, D, F, G, I) The treated or transfected cells were subjected to the migration assay. The quantitative values were expressed as relative migration of the cells by defining the numbers of migrated cells of the untreated group or the untransfected group as 1. Data are represented as the mean ± SD of three-independent experiments. In A and D, $^*P < 0.05$ compared to cells transfected with scrambled shRNA or scrambled siRNA. In B, $^*P < 0.05$ compared to DMSO-treated control cells. In F and I, $^*P < 0.05$ compared to cells transfected with vector control. In G, $^*P < 0.05$ compared to untreated cells.

cells.

3.3. PAR2 induces migration of CL1-5 cells via Gi and Src/p38 MAPK pathways

To determine whether MAPKs are involved in PAR2-mediated migration of CL1-5 cells, we first examined the effect of PAR2 knockdown on the phosphorylation of ERK1/2, p38 MAPK, and c-Jun N-terminal kinase (JNK) in this cell. Knockdown of PAR2 in CL1-5 cells significantly reduced the phosphorylation of ERK1/2 and p38 MAPK but not the phosphorylation of JNK (Fig. 2A). Treatment of CL1-5 cells with PD98059, a MEK1/2 inhibitor which blocks ERK1/2 activation, suppressed the phosphorylation of ERK1/2, while treatment of this cell with SB202190, a p38 MAPK inhibitor, reduced the phosphorylation of mitogen-activated protein kinase-activated protein kinase 2 (MAPKAPK2), a p38 MAPK downstream substrate (Supplementary Fig. S9). These two inhibitors were then used to determine whether ERK1/2 and p38 MAPK signaling are involved in the migration of CL1-5 cells. PD98059 treatment did not affect the cell migration, while SB202190 treatment decreased the cell migration by 58% (Fig. 2B). In addition, treatment of CL1-5 cells with these two inhibitors did not affect the cell viability (Supplementary Fig. S6B). We also examined the effects of knockdown of ERK1/2 on the migration of CL1-5 cells. The expression of ERK1 and ERK2 in the cells transfected with their respective siRNAs was significantly decreased by 50% and 46%, respectively (Fig. 2C). Neither knockdown of ERK1 nor knockdown of ERK2 reduced the migration of CL1-5 cells (Fig. 2D). To further verify the involvement of p38 MAPK signaling in PAR2-mediated migration of CL1-5 cells, we transfected the cells with the plasmid encoding an inducible, dominant-negative mutant of p38 MAPK to examine the effect of its expression on cell migration. When treatment of CL1-5 cells with IPTG to induce the expression of the dominant-negative mutant of p38 MAPK, both the phosphorylation of p38 MAPK and cell migration were reduced (Fig. 2E, F). Thus, p38 MAPK signaling is involved in PAR2-mediated migration of CL1-5 cells.

PAR2-induced MAPK activation is mediated by various G proteins, including Gi, Gq, or G12/13 [8,9]. G proteins may regulate PAR2-mediated cell migration through the activation of p38 MAPK signaling in CL1-5 cells. To test this possibility, we either treated the cells with GP-2A or PTX to block Gq or Gi, respectively, or overexpressed myc-tagged p115-RGS to block G12/13 signaling [58], to determine whether Gq, Gi, or G12/13 contribute to PAR2-mediated migration of CL1-5 cells. The cell migration was significantly reduced by the treatment with PTX but not by the treatment with GP-2A (Fig. 2G). Treatment of CL1-5 cells with PTX and GP-2A did not affect the cell viability (Supplementary Fig. S6B). In addition, overexpression of myc-tagged p115-RGS did not inhibit the cell migration (Fig. 2H, I). These results indicate that PAR2-induced migration of CL1-5 cells is mediated through a Gi-dependent signaling pathway.

Gi-dependent Src activation is required for PAR2-induced chemokinesis in breast cancer cells [59]. To determine whether Src acts downstream of Gi to mediate PAR2-induced migration of CL1-5 cells, we first investigated whether PAR2 knockdown affects Src activation by examining the phosphorylation level of Src at tyrosine 419, an autophosphorylation site of Src. Knockdown of PAR2 in CL1-5 cells significantly reduced the phosphorylation of Src (Supplementary Fig. S10). We then treated the cells with dasatinib, a Src inhibitor, to examine whether Src regulates the migration of CL1-5 cells. Treatment of this cell with dasatinib significantly suppressed the cell migration by 82% (Fig. 3A). In addition, dasatinib treatment did not affect the viability of CL1-5 cells (Supplementary Fig. S6B). To further verify the involvement of Src in PAR2-mediated migration of CL1-5 cells, we overexpressed a kinase-dead Src mutant K298A or a Src double-mutant K298AY419F, which is kinase-dead and autophosphorylation-defective, in CL1-5 cells to examine the effect of their expression on cell migration. Although the phosphorylation of Src at tyrosine 419 in CL1-5 cells overexpressing the kinase-dead Src mutant K298A was increased, the phosphorylation level of Src at tyrosine 419 in cells overexpressing the Src double-mutant K298AY419F was similar to that in cells transfected with the control vector (Fig. 3B). The increased levels of the phosphorylation of Src at tyrosine 419 in CL1-5 cells overexpressing the kinase-dead Src mutant K298A could be due to the phosphorylation of the overexpressed Src mutant K298A at tyrosine 419 by the endogenous Src present in the cells. Overexpression of these two kinase-dead Src mutants, K298A and K298AY419F, did suppress the migration of CL1-5 cells by 79% and 85%, respectively (Fig. 3C). These results indicate that Src is required for PAR2-mediated migration of CL1-5 cells. Since both ERK1/2 and p38 MAPK participate in PAR2-mediated signaling in CL1-5 cells, Src may act as an upstream regulator of these two MAPKs. To test this possibility, we treated the cells with dasatinib to examine its effect on the activation of ERK1/2 and p38 MAPK in CL1-5 cells. Treatment of this cell with dasatinib completely suppressed the phosphorylation of p38 MAPK and Src but not the phosphorylation of ERK1/2 (Fig. 3D). We also overexpressed the two kinase-dead Src mutants, K298A or K298AY419F, in CL1-5 cells to examine their effects on the activation of p38 MAPK. Overexpression of these two kinase-dead Src mutants suppressed the phosphorylation of p38 MAPK in these cells (Fig. 3B). Thus, Src is an upstream modulator of the p38 MAPK signaling pathway in CL1-5 cells. To further determine whether ERK1/2 and Src/p38 MAPK signaling pathways are downstream of Gi in CL1-5 cells, we examined the effect of PTX treatment on the activation of Src, ERK1/2, and p38 MAPK in this cell. PTX Treatment did not reduce the phosphorylation of these three kinases in CL1-5 cells (Fig. 3D). Thus, Gi does not act upstream of ERK1/2 and Src/p38 MAPK signaling pathways in CL1-5 cells. Taken together, these results indicate that PAR2-mediated migration of CL1-5 is regulated by two different signaling pathways. One is the Src/p38 MAPK signaling pathway, and the other is the PTX-sensitive Gi-dependent signaling pathway.

3.4. β-Arrestin 1 is involved in PAR2-mediated migration of CL1-5 cells through the regulation of Src/p38 MAPK signaling pathway

To determine whether β-arrestin 1 and 2 regulate PAR2-mediated cell migration by activation of the Src/p38 MAPK signaling pathway in CL1-5 cells, we examined the effect of knockdown of β-arrestin 1 and 2 on the migration of CL1-5 cells and the activation of Src and p38 MAPK in this cell. The expression of β-arrestin 1 and 2 in cells transfected with the siRNAs targeting their respective β-arrestins was significantly decreased by 43% and 37%, respectively (Fig. 3E). Knockdown of β-arrestin 1 in CL1-5 cells significantly inhibited the cell migration by 72%, while knockdown of β-arrestin 2 had no effect on the migration of CL1-5 cells (Fig. 3F). In addition, knockdown of β-arrestin 1 suppressed the phosphorylation of both Src and p38 MAPK, while knockdown of β-arrestin 2 slightly suppressed the phosphorylation of Src without affecting the phosphorylation of p38 MAPK (Fig. 3E). Thus, β-arrestin 1, not β-arrestin 2, is involved in PAR2-mediated migration of CL1-5 cells by activation of the Src/p38 MAPK signaling pathway.

3.5. Slug mediates PAR2-induced EMT in lung adenocarcinoma cells

In the course of this study, we noted that knockdown of PAR2 resulted in a morphological change of CL1-5 cells. As shown in Fig. 4A, knockdown of PAR2 in CL1-5 cells caused a reduction in the number of elongated, mesenchymal-like cells with a concomitant 1.8-fold increase in the number of round, epithelial-like cells. We further determined whether the morphological changes of CL1-5 cells induced by knockdown of PAR2 are accompanied by the changes in the expression pattern of epithelial and mesenchymal markers. Knockdown of PAR2 induced the expression of E-cadherin, an epithelial marker, and suppressed the expression of N-cadherin and vimentin, mesenchymal markers (Fig. 4B). These results indicate that PAR2 is involved in the process of EMT in CL1-5 cells.

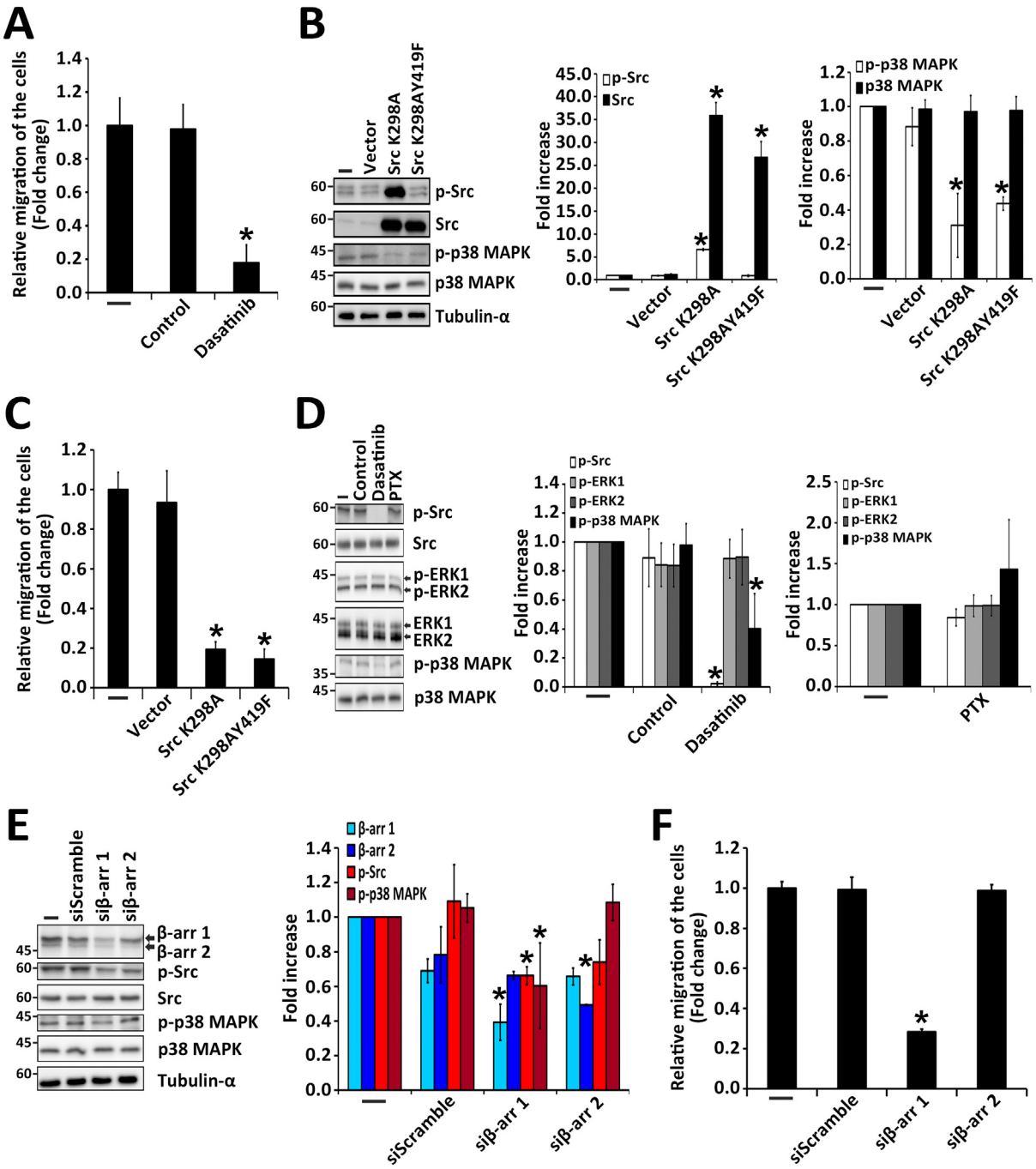

Fig. 3. β-arrestin 1 regulates PAR2-induced migration of CL1-5 cells through the activation of the Src/p38 MAPK signaling pathway. (A) Serum-starved CL1-5 cells were left untreated (−) or treated with 100 nM dasatinib or DMSO (control). (B, C) CL1-5 cells were left untransfected (−) or transfected with the plasmid encoding kinase-dead mutant of Src (Src K298A), kinase-dead and autophosphorylation-defective mutant of Src (Src K298AY419F), or the control vector for 48 h. (D) Serum-starved CL1-5 cells were left untreated (−) or pretreated with 0.1 μg/ml PTX for 16 h, or 100 nM dasatinib or DMSO (control) for 1 h. (E, F) CL1-5 cells were left untransfected (−) or transfected with 200 nM siRNAs specific to β-arrestin 1 (siβ-arr 1) and β-arrestin 2 (siβ-arr 2) or 200 nM scrambled siRNA (siScramble) for 48 h. (A, C, F) The treated or transfected cells were subjected to the migration assay. The quantitative values were expressed as relative migration of the cells by defining the numbers of migrated cells of the untreated group or the untransfected group as 1. Data are represented as the mean ± SD of three-independent experiments. (B, D, E) The cells were lysed and cell lysates were subjected to Western blotting for the detection of the indicated phospho-MAPKs and total MAPKs, phospho-Src, Src, β-arrestin 1, β-arrestin 2, and tubulin-α. The total MAPKs, Src, and tubulin-α were used as loading controls. The quantitative results were expressed as fold increase by defining the amounts of phosphorylated kinases and β-arrestins in untreated or untransfected cells as 1. Data are represented as the mean ± SD of three-independent experiments. In A and D, $^*P < 0.05$ compared to DMSO-treated control cells in dasatinib-treated group (A, D) or untreated cells in PTX-treated group (D). In B and C, $^*P < 0.05$ compared to cells transfected with vector control. In E and F, $^*P < 0.05$ compared to cells transfected with scrambled siRNA.

To identify which EMT-inducing TFs are involved in PAR2-mediated EMT in CL1-5 cells, we employed RT-PCR to examine the effect of PAR2 knockdown on the expression of Snail1, Slug, Snail3, Twist1, Twist2, ZEB1, and ZEB2 in this cell. The mRNA expression of these TFs in PAR2-silenced CL1-5 cells was similar to those in the scrambled control cells (Supplementary Fig. S11). However, knockdown of PAR2 inhibited the protein expression of Slug but not the protein expression of Snail1 and Twist1/2 in CL1-5 cells (Fig. 4C). We further performed qRT-PCR to

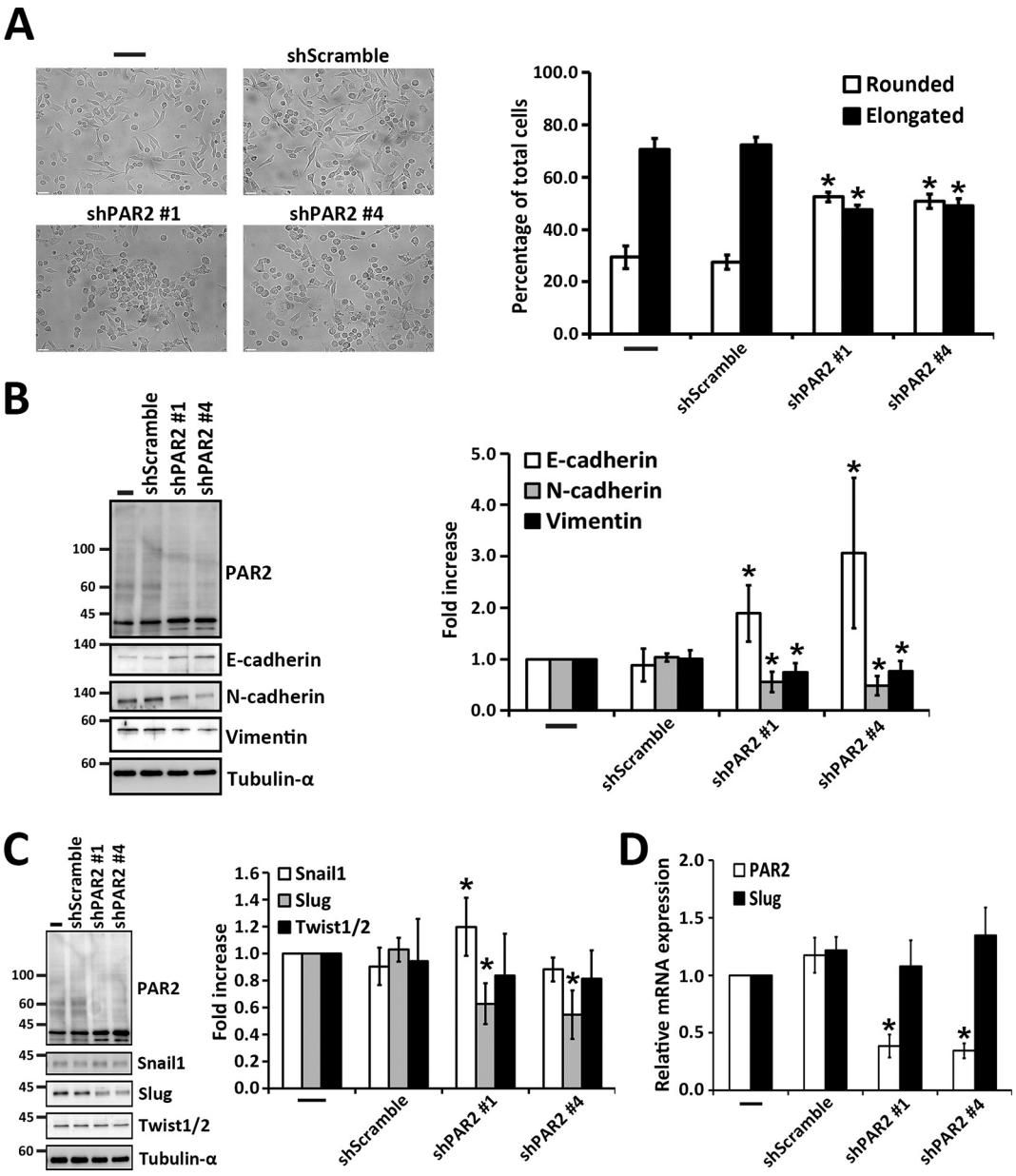

Fig. 4. Knockdown of PAR2 induces MET and reduces Slug expression in CL1-5 cells. CL1-5 cells were left untransfected (−) or transfected with two PAR2-specific shRNAs (shPAR2 #1 and #4) and scrambled shRNA (shScramble) for 48 h. (A) Photomicrographs of the morphology of PAR2-silenced cells were taken by microscope. Scale bar 20 μm. The numbers of the cells with round and elongated shapes were expressed as the percentage of total counted cells. Data are represented as the mean ± SD of three-independent experiments. *$P < 0.05$ compared to cells transfected with scrambled shRNA. (B, C) The cells were lysed and cell lysates were subjected to Western blotting for the detection of PAR2, E-cadherin, N-cadherin, vimentin, Snail1, Slug, Twist1/2, and tubulin-α. The protein bands of PAR2 were detected by the D61D5 antibody. Tubulin-α was used as a loading control. The quantitative results were expressed as fold increase by defining the amounts of EMT makers and EMT-inducing TFs in untransfected cells as 1. Data are represented as the mean ± SD of three-independent experiments. *$P < 0.05$ compared to cells transfected with scrambled shRNA. (D) The cells were lysed and the mRNAs extracted from cell lysates were subjected to the reverse transcription reaction. The mRNA expression of PAR2, Slug, and HPRT1, as a loading control, in these cells was quantified by qRT-PCR. The amounts of mRNA expression of PAR2 and Slug were normalized to that of HPRT1. The quantitative values were expressed as relative mRNA levels by defining the amounts of mRNA expression of PAR2 and Slug in untransfected cells as 1. Data are represented as the mean ± SD of three-independent experiments. *$P < 0.05$ compared to cells transfected with scrambled shRNA.

confirm that the reduced expression of Slug caused by knockdown of PAR2 in CL1-5 cells is at the translational but not transcriptional level. As shown in Fig. 4D, the mRNA expression of Slug was not reduced in PAR2-silenced CL1-5 cells. These results indicate that PAR2 modulates the protein expression of Slug in CL1-5 cells.

Involvement of PAR2 in the process of EMT in CL1-5 cells raises the possibility that the activity of PAR2 may regulate EMT in the cells. We then performed a time course experiment by treating the cells with GB83 or P2pal-18S to examine whether inactivation of PAR2 induces MET in CL1-5 cells. Treatment of cells with GB83 or P2pal-18S increased the percentage of round cells in a time-dependent manner with a nearly 2-fold increase over the control (Fig. 5A, B). At 48 h after treatment of CL1-5 cells with GB83 or P2pal-18S, the expression of E-cadherin was increased and the expression of N-cadherin and vimentin was reduced (Fig. 5C, D). In addition, the expression of Slug in CL1-5 cells was decreased after 6 h of treatment with GB83 or P2pal-18S and then was recovered back to the basal level after the antagonist treatment for 48 h (Fig. 5C, D). Thus, inactivation of PAR2 in CL1-5 cells induces MET that involves down-regulation of Slug expression. We also examined whether activation of PAR2 induces a transition from the

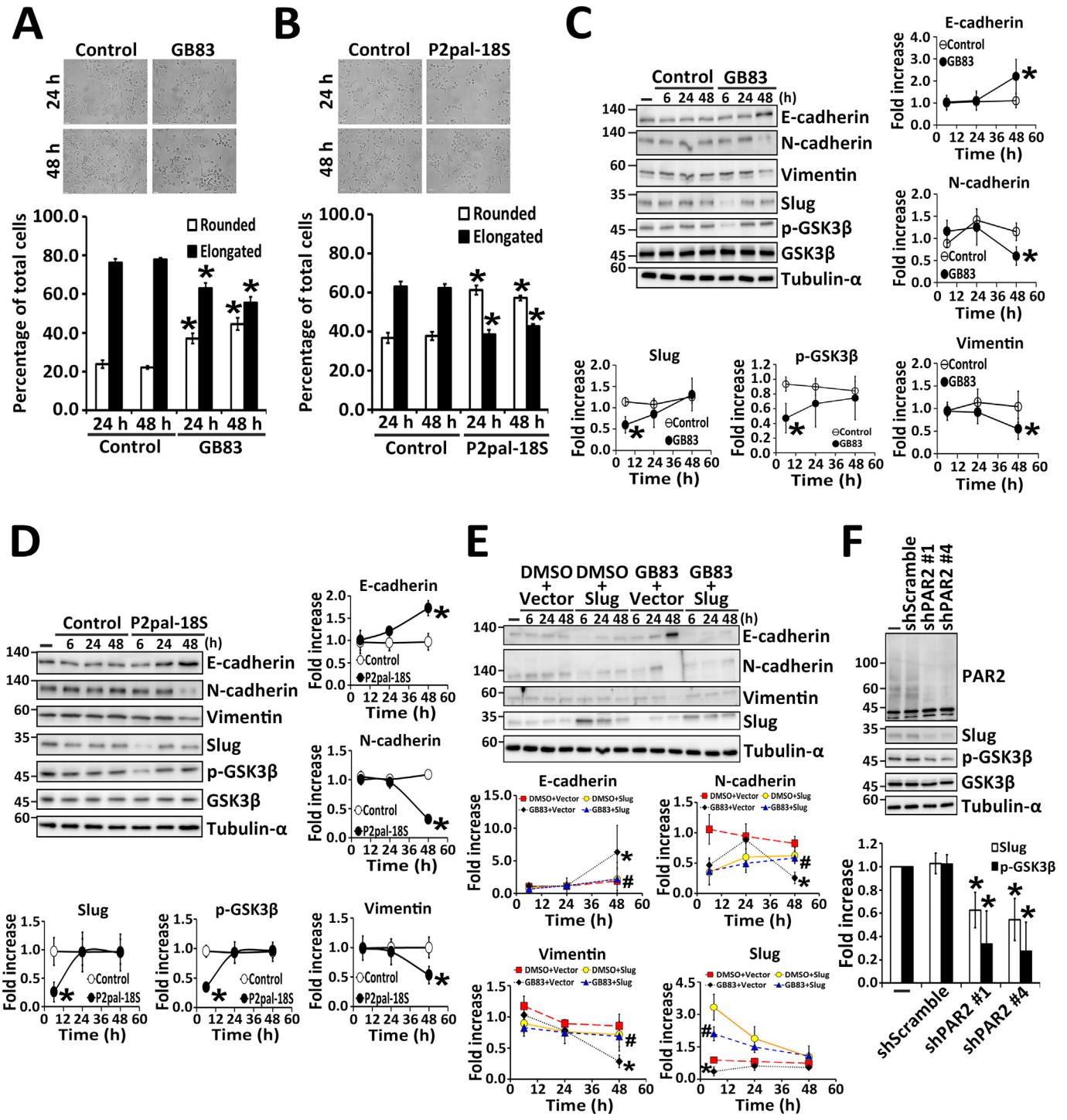

Fig. 5. PAR2 regulates Slug-mediated EMT in CL1-5 cells by inactivating GSK3β. (A–D) CL1-5 cells were left untreated (−) or treated with 50 μM GB83 (A, C), 1 μM P2pal-18S (B, D), or DMSO (control) (A–D) for the indicated times. (E) CL1-5 cells were left untransfected (−) or transfected with the plasmid encoding Slug or the control vector. After 30 h of transfection, these cells were respectively treated with 50 μM GB83 or DMSO for the indicated times. (F) CL1-5 cells were left untransfected (−) or transfected with two PAR2-specific shRNAs (shPAR2 #1 and #4) and scrambled shRNA (shScramble) for 48 h. (A, B) Photomicrographs of the morphology of PAR2-inactivated cells were taken by microscope. Scale bar 20 μm. The numbers of the cells with round and elongated shapes were expressed as the percentage of total counted cells. Data are represented as the mean ± SD of three-independent experiments. (C–F) The cells were lysed and cell lysates were subjected to Western blotting for the detection of PAR2, E-cadherin, N-cadherin, vimentin, Slug, phospho-GSK3β, GSK3β, and tubulin-α. The protein bands of PAR2 were detected by the D61D5 antibody. GSK3β and tubulin-α were used as loading controls. The quantitative results were expressed as fold increase by defining the amounts of Slug, phospho-GSK3β, and EMT makers in untreated or untransfected cells as 1. Data are represented as the mean ± SD of three-independent experiments. In A–D, $^{*}P < 0.05$ compared to DMSO-treated control cells at the same time point. In E, $^{*}P < 0.05$ compared to DMSO-treated cells transfected with the control vector at the same time point; $^{\#}P < 0.05$ compared to GB83-treated cells transfected with the control vector at the same time point. In F, $^{*}P < 0.05$ compared to cells transfected with scrambled shRNA.

epithelial-like morphology to the mesenchymal-like morphology in lung adenocarcinoma H1299 cells. Stimulation of H1299 cells with SLIGKV-NH_2 or 2f-LI caused a time-dependent increase in the number of elongated cells (Supplementary Fig. S7E). After 24 and 48 h of stimulation, the expression of E-cadherin was decreased and the expression of N-cadherin was increased in H1299 cells (Supplementary Fig. S7F). In addition, the expression of Slug and vimentin was increased in cells stimulated with SLIGKV-NH_2 or 2f-LI for 6, 24, and 48 h (Supplementary Fig. S7F). When H1299 cells were treated with the negative control peptide, VKGILS-NH_2, the cell morphology and the expression of the EMT markers were not changed (Supplementary Fig. S7E, F). These results indicate that activation of PAR2 induces Slug-mediated EMT in H1299 cells. Thus, Slug regulates PAR2-mediated EMT in both CL1-5 and H1299 cells.

3.6. ERK2 participates in Slug-dependent EMT induced by PAR2 through the inhibition of glycogen synthase kinase 3β in CL1-5 cells

To evaluate whether Slug plays a role in PAR2-mediated EMT of CL1-5 cells, we examined whether overexpression of Slug is able to reverse MET induced by knockdown and inactivation of PAR2 in this cell. When Slug was overexpressed in PAR2-silenced CL1-5 cells, the expression of E-cadherin was reduced and the expression of N-cadherin and vimentin was increased as compared to those in the cells transfected with the control vector (Supplementary Fig. S12). In CL1-5 cells treated with GB83 for 48 h, overexpression of Slug also reversed the expression levels of E-cadherin, N-cadherin, and vimentin (Fig. 5E). The expression levels of these EMT markers in Slug-overexpressed CL1-5 cells treated with GB83 was similar to that in Slug-overexpressed cells treated with DMSO (Fig. 5E). The loss of Slug expression induced by GB83 treatment at 6 h did not occur in Slug-overexpressed cells due to the exogenous expression of Slug (Fig. 5E). Thus, Slug plays a key role in regulating PAR2-mediated EMT in CL1-5 cells.

It has been reported that activation of GSK3β by reducing its phosphorylated level at Ser9 can induce Slug degradation [60,61]. To determine whether PAR2 modulates Slug expression through regulating GSK3β activity in CL1-5 cells, we examined the effects of knockdown and inactivation of PAR2 on the phosphorylation of GSK3β at Ser9 in this cell. Knockdown of PAR2 in CL1-5 cells markedly reduced the phosphorylation of GSK3β at Ser9 and the expression of Slug (Fig. 5F). The phosphorylation of GSK3β at Ser9 and the expression of Slug were decreased in CL1-5 cells after treatment with GB83 or P2pal-18S for 6 h (Fig. 5C, D). These results indicate that PAR2 negatively regulates the activity of GSK3β in CL1-5 cells. Also, the GSK3β activity is inversely correlated to the expression of Slug in this cell. We further treated the cells with TWS119, an inhibitor of GSK3β, to examine whether inactivation of GSK3β is able to reverse MET induced by PAR2 knockdown in CL1-5 cells. In the scrambled control cells, treatment of CL1-5 cells with TWS119 did not affect the basal expression of EMT markers, Slug, and the phosphorylation of Ser9 of GSK3β (Supplementary Fig. S13). However, treatment of PAR2-silenced CL1-5 cells with TWS119 reduced the expression of E-cadherin, recovered the expression of N-cadherin, vimentin, and Slug, and increased the phosphorylation of Ser9 of GSK3β (Supplementary Fig. S13). Taken together, these results indicate that the constitutive activation of PAR2 suppresses the activity of GSK3β to maintain Slug expression and further induces the mesenchymal-like morphology in CL1-5 cells.

ERK1/2 and p38 MAPK down-regulate the activity of GSK3β by increasing the phosphorylation capacity of GSK3β at Ser9 [62,63]. PAR2 may activate ERK1/2 or p38 MAPK to regulate EMT in CL1-5 cells. We performed a time-course experiment to examine whether inactivation of ERK1/2 or p38 MAPK induces MET in CL1-5 cells. Treatment of CL1-5 cells with PD98059 for 24 and 48 h induced cell rounding (Fig. 6A). After 48 h of treatment with PD98059, the expression of E-cadherin was markedly increased and the expression of N-cadherin and vimentin was significantly decreased in CL1-5 cells as compared to those in the control cells (Fig. 6B). However, treatment with SB202190 did not affect the cell morphology, decrease the expression of N-cadherin and vimentin, and increase the expression of E-cadherin in CL1-5 cells (Fig. 6C, D). Overexpression of an inducible, dominant-negative mutant of p38 MAPK in this cell also did not affect the cell morphology and the expression of the EMT markers in CL1-5 cells (Fig. 6E, F). These results indicate that ERK1/2, not p38 MAPK, is involved in PAR2-mediated EMT in CL1-5 cells. In addition, treatment of CL1-5 cells with PD98059 for 6 h resulted in the reduction of Slug and this reduction coincided with the decrease of the phosphorylation of GSK3β at Ser9 (Fig. 6B). Thus, ERK1/2 induce the inactivation of GSK3β to mediate Slug-dependent EMT induced by PAR2 in CL1-5 cells.

Activation of ERK1/2 can suppress the activity of GSK3β by induction of the phosphorylation of Ser9 in GSK3β [62]. Our finding that inactivation of MEK1/2, upstream of ERK1/2, by PD98059 induced GSK3β activation in CL1-5 cells indicates that MEK1/ERK1 and MEK2/ERK2 signaling pathways are involved in regulating GSK3β activity in PAR2-mediated EMT in CL1-5 cells. To further determine whether ERK1 or ERK2 regulate EMT in CL1-5 cells, we examined the effects of knockdown of ERK1 or ERK2 on the cell morphology and the expression of EMT markers in these cells. Knockdown of ERK1 in CL1-5 cells did not induce the change of cell morphology, whereas knockdown of ERK2 in this cell induced cell rounding (Fig. 7A). Knockdown of ERK1 suppressed the expression of E-cadherin and induced the expression of N-cadherin, vimentin, Slug, and the phosphorylation of GSK3β at Ser9 (Fig. 7B). However, knockdown of ERK2 induced the expression of E-cadherin and suppressed the expression of N-cadherin, vimentin, Slug, and the phosphorylation of GSK3β at Ser9 (Fig. 7B). Although knockdown of ERK1 and knockdown of ERK2 oppositely regulate the expression of EMT markers in CL1-5 cells, only knockdown of ERK2 induces the change of cell morphology to an epithelial-like phenotype. This finding indicates that ERK2 is involved in PAR2-mediated EMT in CL1-5 cell. To further verify whether ERK2 regulates PAR2-mediated EMT in CL1-5 cells, we overexpressed constitutively active MEK2 in CL1-5 cells to investigate whether constitutive activation of MEK2 suppresses GSK3β activity by induction of the phosphorylation of GSK3β at Ser9 to counteract MET induced by inactivation of PAR2 in this cell. After 6 h of treatment with GB83, the expression of Slug and the phosphorylation of GSK3β at Ser9 were increased in MEK2-overexpressed CL1-5 cells as compared to those in MEK2-overexpressed CL1-5 cells treated with DMSO (Fig. 7C). In addition, overexpression of constitutively active MEK2 recovered the expression of N-cadherin and vimentin and reduced the expression of E-cadherin in cells treated with GB83 for 48 h (Fig. 7C). Thus, MEK2-dependent ERK2 activation contributes to PAR2-mediated EMT of CL1-5 cells through the inactivation of GSK3β to stabilize Slug expression.

3.7. High expression of PAR2 is correlated with poor survival of patients with lung adenocarcinoma

Since PAR2 promotes EMT, migration, and invasion in lung adenocarcinoma cells, a Kaplan–Meier survival analysis of patients with lung adenocarcinoma was conducted to determine the prognostic significance of PAR2 expression. We found that a high expression level of PAR2 is correlated with poor overall survival and reduced recurrence free survival of the cancer patients (Fig. 8). These data suggest the utility of PAR2 as a prognostic biomarker in monitoring lung cancer progression.

4. Discussion

Our study shows that PAR2 not only induces migration but also promotes Slug-mediated EMT in lung adenocarcinoma cells. PAR2-induced migration of CL1-5 cells is mediated by β-arrestin 1-dependent activation of the Src/p38 MAPK signaling pathway, whereas PAR2-induced EMT in CL1-5 cells is regulated by ERK2-mediated Slug

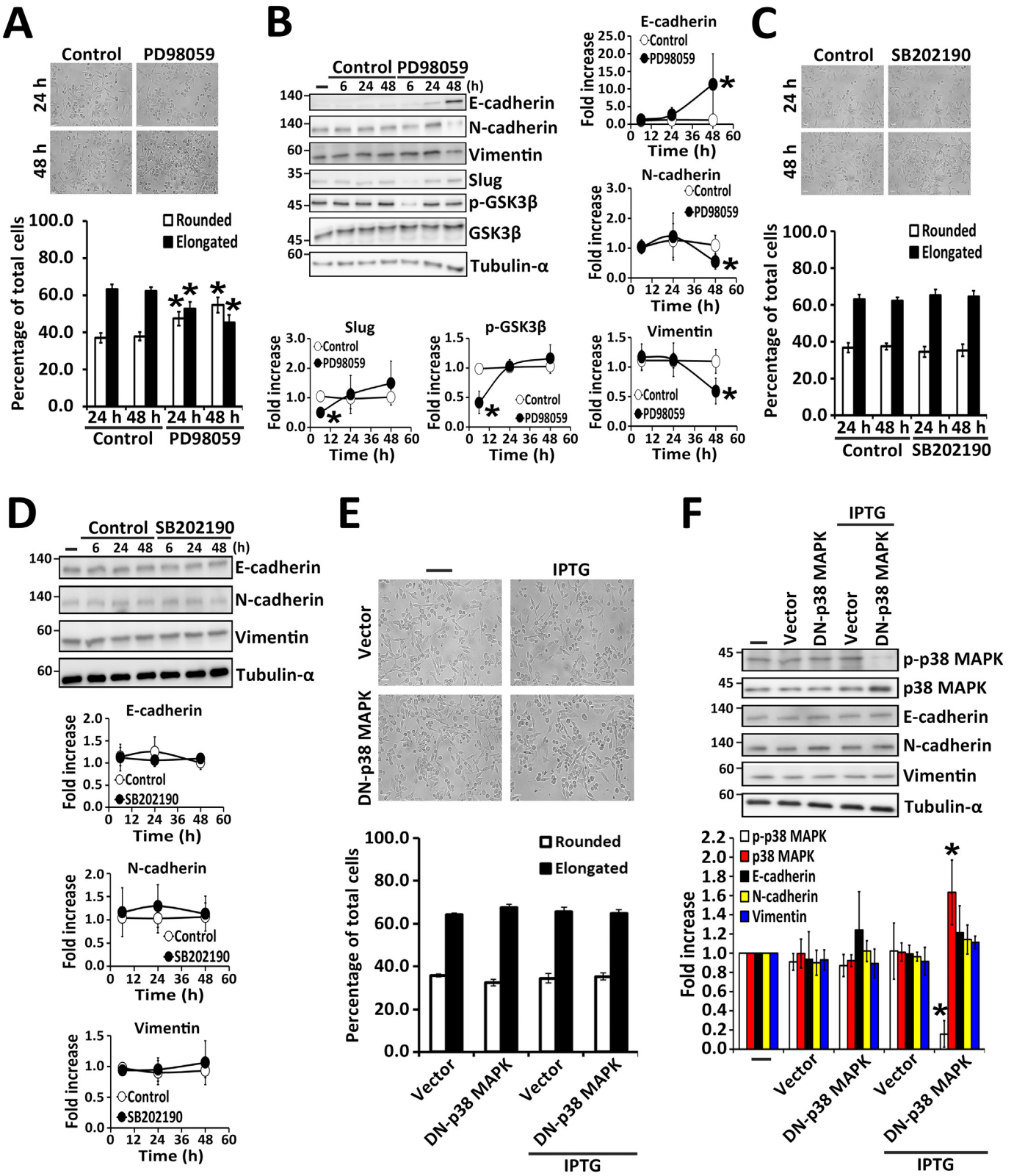

Fig. 6. Inactivation of ERK1/2 suppresses Slug-mediated EMT in CL1-5 cells. (A–D) CL1-5 cells were left untreated (−) or treated with 15 μM PD98059 (A, B), 20 μM SB202190 (C, D), or DMSO (control) (A–D) for the indicated times. (E, F) CL1-5 cells were left untransfected (−) or transfected with the plasmid encoding an inducible dominant-negative mutant of p38 MAPK (DN-p38 MAPK) or the control vector. After 24 h of transfection, these cells were left untreated or treated with 5 mM IPTG for 48 h. (A, C, E) Photomicrographs of the morphology of ERK1/2- or p38 MAPK-inactivated cells were taken by microscope. Scale bar 20 μm. The numbers of the cells with round and elongated shapes were expressed as the percentage of total counted cells. Data are represented as the mean ± SD of three-independent experiments. (B, D, F) The cells were lysed and cell lysates were subjected to Western blotting for the detection of E-cadherin, N-cadherin, vimentin, Slug, phospho-GSK3β, GSK3β, phospho-p38 MAPK, p38 MAPK, and tubulin-α. GSK3β and tubulin-α were used as loading controls. The quantitative results were expressed as fold increase by defining the amounts of Slug, phospho-GSK3β, phospho-p38 MAPK, p38 MAPK, and EMT makers in untreated or untransfected cells as 1. Data are represented as the mean ± SD of three-independent experiments. In A–D, $^*P < 0.05$ compared to DMSO-treated control cells at the same time point. In E and F, $^*P < 0.05$ compared to untreated cells transfected with DN-p38 MAPK.

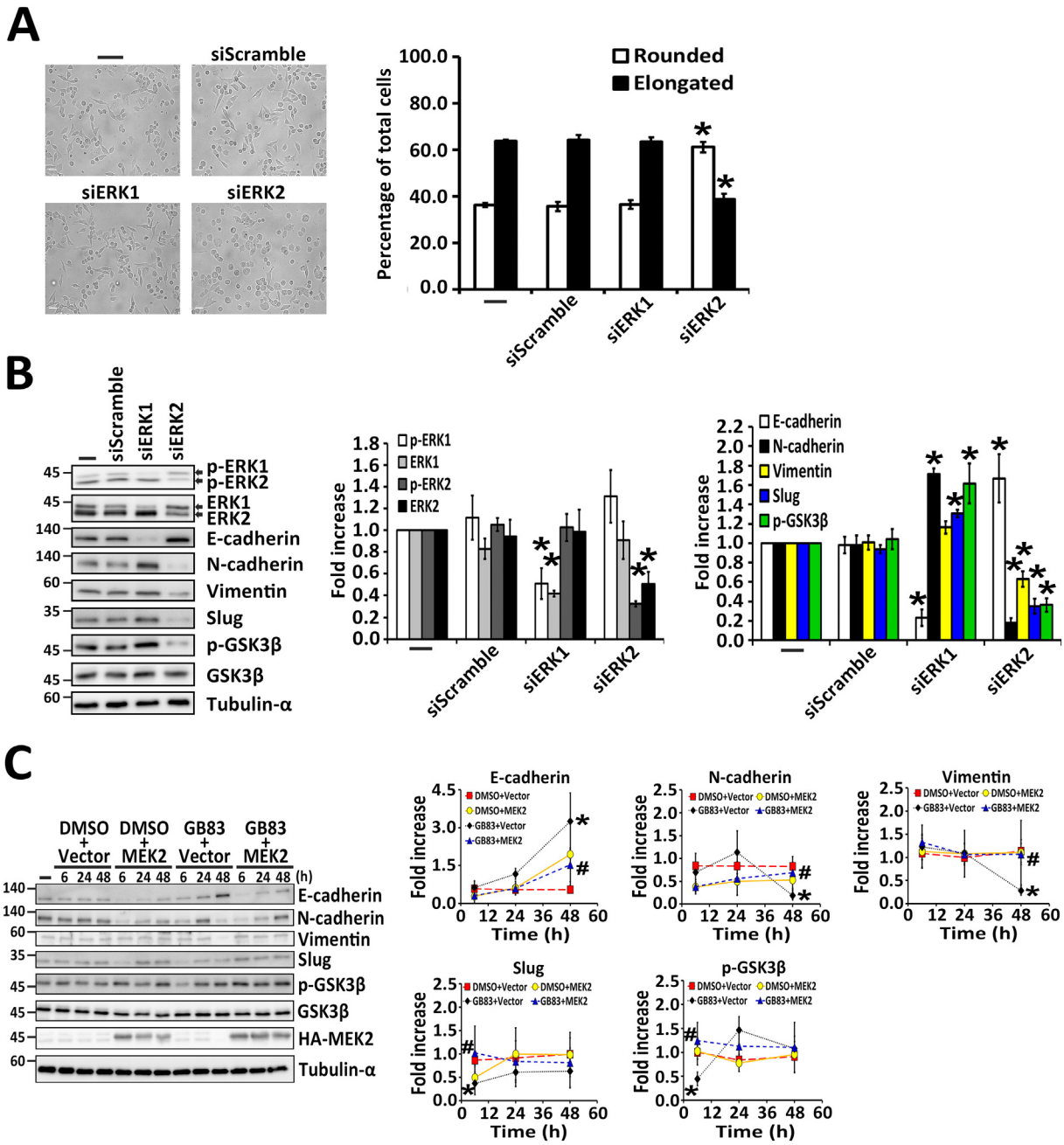

Fig. 7. PAR2 activates ERK2 to induce EMT in CL1-5 cells by inactivating GSK3β. (A, B) CL1-5 cells were left untransfected (−) or transfected with 200 nM siRNAs specific to ERK1 and ERK2 or 200 nM scrambled siRNA (siScramble) for 48 h. (C) CL1-5 cells were left untransfected (−) or transfected with the plasmid encoding HA-tagged MEK2 or the control vector. After 30 h of transfection, the cells were respectively treated with 50 μM GB83 or DMSO for the indicated times. (A) Photomicrographs of the morphology of ERK1- or ERK2-silenced cells were taken by microscope. Scale bar 20 μm. The numbers of the cells with round and elongated shapes were expressed as the percentage of total counted cells. Data are represented as the mean ± SD of three-independent experiments. (B, C) The cells were lysed and cell lysates were subjected to Western blotting for the detection of phospho-ERK1/2, ERK1/2, E-cadherin, N-cadherin, vimentin, Slug, phospho-GSK3β, GSK3β, HA-MEK2, and tubulin-α. ERK1/2, GSK3β, and tubulin-α were used as loading controls. The quantitative results were expressed as fold increase by defining the amounts of phospho-ERK1/2, ERK1/2, Slug, phospho-GSK3β, and EMT makers in untransfected cells as 1. Data are represented as the mean ± SD of three-independent experiments. In A and B, $^{*}P < 0.05$ compared to cells transfected with scrambled siRNA. In C, $^{*}P < 0.05$ compared to DMSO-treated cells transfected with the control vector at the same time point; $^{\#}P < 0.05$ compared to GB83-treated cells transfected with the control vector at the same time point.

stabilization. Further, GSK3β acts downstream of ERK2 as a negative regulator to modulate Slug expression in this PAR2-mediated EMT process. Here, we provide the first evidence that PAR2 induces Slug-mediated EMT in lung adenocarcinoma cells. PAR2 may play a critical role in metastasis of lung adenocarcinoma by promoting EMT and migration of lung cancer cells. Our study also reveals that the high expression of PAR2 is correlated with a poor prognosis in lung adenocarcinoma patients. The expression of PAR2 may be used to predict the prognosis of patients with lung adenocarcinoma.

In contrast to our finding that PAR2 mediates EMT and migration of lung adenocarcinoma cells through different MAPK signaling pathways, activation of enzyme-linked receptors regulates EMT and cell migration through a shared signaling pathway. For example, TGF-β receptor, the key inducer for EMT, promotes EMT and cell migration through the phosphatidylinositol 3-kinase (PI3K)/Akt signaling pathway [64]. Unlike enzyme-linked receptors, different signaling pathways are involved

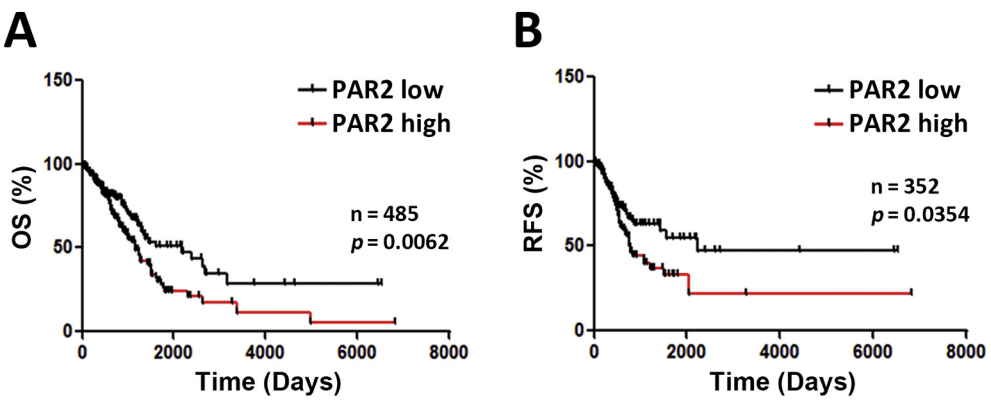

Fig. 8. The high expression of PAR2 is correlated with a poor prognosis in lung adenocarcinoma. Kaplan–Meier analysis was used to estimate the overall survival (OS) (A) and recurrent free survival (RFS) (B) among TCGA LUAD patients according to the expression of PAR2. Comparative analysis between the two groups was performed by log-rank test.

in GPCR-induced EMT and migration of cancer cells. In breast cancer cells, angiotensin II type I receptor, a GPCR, induces EMT through Src-dependent EGFR transactivation and mediates migration via PI3K/Akt-dependent activation of NF-κB [65,66]. In lung cancer cells, PAR1 induces EMT through PKC-dependent ERK1/2 activation and mediates migration via the activation of the PI3K/Akt pathway [42,67]. For a specific GPCR, the different signaling pathways can be induced by its biased ligands [68]. It is possible that proteases secreted from CL1-5 cells cleave at the non-canonical cleavage sites of PAR2 to create biased ligands to induce biased signaling. The different MAPK signaling pathways which regulate PAR2-mediated EMT and cell migration may be induced by the biased ligands generated by proteases.

Proteases secreted by the lung cancer cells or the neighboring non-cancer cells are thought to regulate the EMT and cell migration of lung cancer. Our study shows that serine proteases, cysteine proteases, and MMPs secreted by CL1-5 cells may constitutively activate PAR2 to induce migration and invasion of CL1-5 cells. Although these three proteases are involved in the migration and invasion of CL1-5 cells, treatment of this cell with the serine proteases inhibitor, PMSF, caused the greatest inhibitory effect on its migration and invasion. These results suggest that serine proteases secreted by CL1-5 cells could be a main contributor to activate PAR2 constitutively and to further induce PAR2-mediated EMT in this mesenchymal-like cell. Unlike CL1-5 cells, agonist-stimulation of PAR2 promotes migration and EMT in epithelial-like H1299 cells. These findings suggest that PAR2-induced migration and EMT in lung cancer cells may also be mediated by paracrine secretion of serine proteases by neighboring non-cancerous cells in the tumor microenvironment. It has been reported that tissue factor and coagulation factor VIIa released form the microvesicles secreted by glioblastoma multiforme cells activate PAR2 and then induce angiogenesis in neighboring endothelial cells to facilitate cancer growth [69]. An in vivo study shows that PAR2 knockout mice delayed the development of breast tumor and decreased spontaneous lung metastasis in response to the activation of tissue factor and coagulation factor VIIa [70]. Our data, together with the previous findings just mentioned, support the idea that serine proteases may play a role in PAR2-induced lung cancer progression through the mutual interaction between cancer cells and non-cancerous cells in the tumor microenvironment.

PAR2 induces migration of breast cancer cells through both G protein and β-arrestin signaling pathways. In MDA-MB-231 cells, Gi and β-arrestins mediate PAR2-induced cell migration through the activation of JNK and ERK1/2, respectively [59,71]. As shown in our study, both Gi and β-arrestin 1 regulate PAR2-mediated migration of CL1-5 cells. β-arrestin 1 regulates PAR2-mediated cell migration through the activation of the Src/p38 MAPK signaling pathway. This is the first study to show that p38 MAPK is involved in β-arrestin 1-dependent cell migration induced by PAR2. In contrast to the report that β-arrestin 1 and 2 co-regulate PAR2-mediated migration of breast cancer cells [71], our study shows that β-arrestin 2 is not involved in the migration of CL1-5 cells. Accumulating evidence has demonstrated that β-arrestin 1 and 2 regulate different molecular and cellular events, such as phosphorylation-dependent or -independent internalization of δ-opioid receptor, activation or degradation of Src induced by PAR1, degranulation of mast cell or generation of chemokine C—C motif chemokine ligand 4 (CCL4) induced by C3a receptor [72–74]. Thus, β-arrestin 1 and 2 may be differentially required for PAR2-mediated responses in lung adenocarcinoma cells. Apart from β-arrestin 1, the Gi-dependent pathway also contributes to PAR2-mediated migration of CL1-5 cells. The finding that Src, ERK1/2, and p38 MAPK do not act downstream of Gi in CL1-5 cells indicates that other molecules are involved in Gi-dependent cell migration induced by PAR2. Previous studies reported that PTX-sensitive Gi mediates cell migration through the activation of PI3K/Akt and Rho GTPases [75,76]. However, whether Gi activates PI3K/Akt or Rho GTPase to mediate PAR2-induced cell migration needs to be further investigated.

In summary, PAR2 induces migration and Slug-mediated EMT in lung adenocarcinoma CL1-5 and H1299 cells. In CL1-5 cells, PAR2 promotes migration through the activation of p38 MAPK. ERK2 stabilizes Slug expression by suppressing the activity of GSK3β in PAR2-mediated EMT process. PAR2 may play a key role in regulating metastasis in lung adenocarcinoma.

5. Conclusions

This study shows that PAR2 induces migration and EMT in lung adenocarcinoma cells. β-arrestin 1-mediated activation of p38 MAPK is responsible for PAR2-induced migration of CL1-5 cells, whereas ERK2-mediated stabilization of Slug is essential for PAR2-induced EMT in this cell. Furthermore, a poor prognosis in patients with lung adenocarcinoma correlates with the high expression of PAR2. PAR2 might serve as a potential therapeutic target in the treatment of metastatic lung adenocarcinoma and a prognostic marker in patients with lung adenocarcinoma.

Funding

This work was supported by the Ministry of Science and Technology of Taiwan [MOST 107-2311-B-007-004, MOST 104-2311-B-007-003, NSC101-2311-B-007-007, and NSC98-2311-B-007-006-MY3] and the research program of National Tsing Hua University [104N2052E1, 105N528CE1, and 106N528CE1]. The funders had no role in study design, data collection and analysis, decision to publish, or preparation of the manuscript.

Conflict of interest

The authors declare no potential conflicts of interest.

Authors' contributions

The conception and design of the study: C-C. Tsai and H-W. Fu.

Acquisition of data: C-C. Tsai.

Analysis and interpretation of data: C-C. Tsai, Y-T. Chou, and H-W. Fu.

Drafting the article: C-C. Tsai.

Revising the article critically for important intellectual content: Y-T. Chou and H-W. Fu.

Final approval of the version to be submitted: C-C. Tsai, Y-T. Chou, and H-W. Fu.

Transparency document

The Transparency document associated with this article can be found, in online version.

Acknowledgements

We appreciate Dr. Cheng-Wen Wu at the Institute of Biomedical Sciences, Academia Sinica, Taipei, Taiwan, for providing lung adenocarcinoma cell lines CL1-0 and CL1-5. We thank Dr. Shaun Coughlin at University of California, San Francisco (UCSF), San Francisco, California, USA, for providing cDNA encoding Flag-tagged PAR2 in the pBJ mammalian expression vector, Dr. Amira Klip at Hospital for Sick Children, Toronto, Canada, for providing cDNA encoding an inducible, dominant-negative mutant of p38 MAPK (T180AG181GY182F) in the pOP13 mammalian expression vector, Dr. Patrick Casey at Duke-NUS Graduate Medical School, Singapore, for providing cDNA encoding p115-RGS in the pCMV5-myc mammalian expression vector, Dr. Masanori Hatakeyama at Hokkaido University, Japan, for providing cDNA encoding kinase-dead Src (K298A) and kinase-dead autophosphorylation-defective Src (K298AY419F) in the PSP65SRα mammalian expression vector, Dr. Muh-Hwa Yang at National Yang-Ming University, Taipei, Taiwan, for providing cDNA encoding wild-type Slug in the pcDNA3.1 (+) mammalian expression vector, and Dr. Yun-Wei Lin at National Chiayi University, Chiayi, Taiwan, for providing cDNA encoding HA-tagged constitutively active MEK2 in the pcDNA3 mammalian expression vector. We are grateful to Dr. Chiou-Hwa Yuh at National Health Research Institutes, Zhunan, Taiwan, for providing tunicamycin. We also thank the colleagues in the College of Life Science at National Tsing Hua University, Taiwan, for providing the research materials: Dr. Jia-Ling Yang for providing siRNAs targeting human ERK1 and ERK2, Dr. Ming-Der Perng for providing antibodies against p38 MAPK and JNK, Dr. I-Ching Wang for providing the anti-Snail1 antibody, Dr. Jia-Lin Lee for providing the antibody against Twist1/2 and the primer for Twist 1, Dr. Lih-Yuan Lin for providing MAPKs inhibitors, and Dr. Chung-Yu Lan for providing PCR-related reagents.

Appendix A. Supplementary data

Supplementary data to this article can be found online at https://doi.org/10.1016/j.bbamcr.2018.10.011.

References

[1] L.A. Torre, F. Bray, R.L. Siegel, J. Ferlay, J. Lortet-Tieulent, A. Jemal, Global cancer statistics, 2012, CA Cancer J. Clin. 65 (2015) 87–108.
[2] S. Rakashanda, F. Rana, S. Rafiq, A. Masood, S. Amin, Role of proteases in cancer: a review, Biotechnol. Mol. Biol. Rev. 7 (2012) 12.
[3] H.V. Nathalie, P. Chris, G. Serge, C. Catherine, B. Benjamin, B. Claire, P. Christelle, L. Briollais, R. Pascale, J. Marie-Lise, C. Yves, High kallikrein-related peptidase 6 in non-small cell lung cancer cells: an indicator of tumour proliferation and poor prognosis, J. Cell. Mol. Med. 13 (2009) 4014–4022.
[4] N. Kawano, H. Osawa, T. Ito, Y. Nagashima, F. Hirahara, Y. Inayama, Y. Nakatani, S. Kimura, H. Kitajima, N. Koshikawa, K. Miyazaki, H. Kitamura, Expression of gelatinase A, tissue inhibitor of metalloproteinases-2, matrilysin, and trypsin(ogen) in lung neoplasms: an immunohistochemical study, Hum. Pathol. 28 (1997) 613–622.
[5] H. Yamamoto, S. Iku, Y. Adachi, A. Imsumran, H. Taniguchi, K. Nosho, Y. Min, S. Horiuchi, M. Yoshida, F. Itoh, K. Imai, Association of trypsin expression with tumour progression and matrilysin expression in human colorectal cancer, J. Pathol. 199 (2003) 176–184.
[6] M.N. Adams, R. Ramachandran, M.K. Yau, J.Y. Suen, D.P. Fairlie, M.D. Hollenberg, J.D. Hooper, Structure, function and pathophysiology of protease activated receptors, Pharmacol. Ther. 130 (2011) 248–282.
[7] S. Nystedt, K. Emilsson, A.K. Larsson, B. Strombeck, J. Sundelin, Molecular cloning and functional expression of the gene encoding the human proteinase-activated receptor 2, Eur. J. Biochem. 232 (1995) 84–89.
[8] M. Schultheiss, B. Neumcke, H.P. Richter, Endogenous trypsin receptors in Xenopus oocytes: linkage to internal calcium stores, Cell. Mol. Life Sci. 53 (1997) 842–849.
[9] K.L. McCoy, S.F. Traynelis, J.R. Hepler, PAR1 and PAR2 couple to overlapping and distinct sets of G proteins and linked signaling pathways to differentially regulate cell physiology, Mol. Pharmacol. 77 (2010) 1005–1015.
[10] L. Stalheim, Y. Ding, A. Gullapalli, M.M. Paing, B.L. Wolfe, D.R. Morris, J. Trejo, Multiple independent functions of arrestins in the regulation of protease-activated receptor-2 signaling and trafficking, Mol. Pharmacol. 67 (2005) 78–87.
[11] M. Molino, E.S. Barnathan, R. Numerof, J. Clark, M. Dreyer, A. Cumashi, J.A. Hoxie, N. Schechter, M. Woolkalis, L.F. Brass, Interactions of mast cell tryptase with thrombin receptors and PAR-2, J. Biol. Chem. 272 (1997) 4043–4049.
[12] E. Camerer, W. Huang, S.R. Coughlin, Tissue factor- and factor X-dependent activation of protease-activated receptor 2 by factor VIIa, Proc. Natl. Acad. Sci. U. S. A. 97 (2000) 5255–5260.
[13] R. Smith, A. Jenkins, A. Lourbakos, P. Thompson, V. Ramakrishnan, J. Tomlinson, U. Deshpande, D.A. Johnson, R. Jones, E.J. Mackie, R.N. Pike, Evidence for the activation of PAR-2 by the sperm protease, acrosin: expression of the receptor on oocytes, FEBS Lett. 484 (2000) 285–290.
[14] K.K. Hansen, P.M. Sherman, L. Cellars, P. Andrade-Gordon, Z. Pan, A. Baruch, J.L. Wallace, M.D. Hollenberg, N. Vergnolle, A major role for proteolytic activity and proteinase-activated receptor-2 in the pathogenesis of infectious colitis, Proc. Natl. Acad. Sci. U. S. A. 102 (2005) 8363–8368.
[15] T. Takeuchi, J.L. Harris, W. Huang, K.W. Yan, S.R. Coughlin, C.S. Craik, Cellular localization of membrane-type serine protease 1 and identification of protease-activated receptor-2 and single-chain urokinase-type plasminogen activator as substrates, J. Biol. Chem. 275 (2000) 26333–26342.
[16] S. Wilson, B. Greer, J. Hooper, A. Zijlstra, B. Walker, J. Quigley, S. Hawthorne, The membrane-anchored serine protease, TMPRSS2, activates PAR-2 in prostate cancer cells, Biochem. J. 388 (2005) 967–972.
[17] A.J. Ramsay, J.C. Reid, M.N. Adams, H. Samaratunga, Y. Dong, J.A. Clements, J.D. Hooper, Prostatic trypsin-like kallikrein-related peptidases (KLKs) and other prostate-expressed tryptic proteinases as regulators of signalling via proteinase-activated receptors (PARs), Biol. Chem. 389 (2008) 653–668.
[18] A.J. Ramsay, Y. Dong, M.L. Hunt, M. Linn, H. Samaratunga, J.A. Clements, J.D. Hooper, Kallikrein-related peptidase 4 (KLK4) initiates intracellular signaling via protease-activated receptors (PARs). KLK4 and PAR-2 are co-expressed during prostate cancer progression, J. Biol. Chem. 283 (2008) 12293–12304.
[19] K. Oikonomopoulou, K.K. Hansen, M. Saifeddine, N. Vergnolle, I. Tea, M. Blaber, S.I. Blaber, I. Scarisbrick, E.P. Diamandis, M.D. Hollenberg, Kallikrein-mediated cell signalling: targeting proteinase-activated receptors (PARs), Biol. Chem. 387 (2006) 817–824.
[20] A. Lourbakos, C. Chinni, P. Thompson, J. Potempa, J. Travis, E.J. Mackie, R.N. Pike, Cleavage and activation of proteinase-activated receptor-2 on human neutrophils by gingipain-R from *Porphyromonas gingivalis*, FEBS Lett. 435 (1998) 45–48.
[21] S.B. Elmariah, V.B. Reddy, E.A. Lerner, Cathepsin S signals via PAR2 and generates a novel tethered ligand receptor agonist, PLoS One 9 (2014) e99702.
[22] P. Zhao, T. Lieu, N. Barlow, M. Metcalf, N.A. Veldhuis, D.D. Jensen, M. Kocan, S. Sostegni, S. Haerteis, V. Baraznenok, I. Henderson, E. Lindstrom, R. Guerrero-Alba, E.E. Valdez-Morales, W. Liedtke, P. McIntyre, S.J. Vanner, C. Korbmacher, N.W. Bunnett, Cathepsin S causes inflammatory pain via biased agonism of PAR2 and TRPV4, J. Biol. Chem. 289 (2014) 27215–27234.
[23] R. Ramachandran, K. Mihara, H. Chung, B. Renaux, C.S. Lau, D.A. Muruve, K.A. DeFea, M. Bouvier, M.D. Hollenberg, Neutrophil elastase acts as a biased agonist for proteinase-activated receptor-2 (PAR2), J. Biol. Chem. 286 (2011) 24638–24648.
[24] M. Moilanen, T. Sorsa, M. Stenman, P. Nyberg, O. Lindy, J. Vesterinen, A. Paju, Y.T. Konttinen, U.H. Stenman, T. Salo, Tumor-associated trypsinogen-2 (trypsinogen-2) activates procollagenases (MMP-1, -8, -13) and stromelysin-1 (MMP-3) and degrades type I collagen, Biochemistry 42 (2003) 5414–5420.
[25] P. Nyberg, M. Moilanen, A. Paju, A. Sarin, U.H. Stenman, T. Sorsa, T. Salo, MMP-9 activation by tumor trypsin-2 enhances in vivo invasion of human tongue carcinoma cells, J. Dent. Res. 81 (2002) 831–835.
[26] X. Li, H.H. Tai, Thromboxane A2 receptor-mediated release of matrix metalloproteinase-1 (MMP-1) induces expression of monocyte chemoattractant protein-1 (MCP-1) by activation of protease-activated receptor 2 (PAR2) in A549 human lung adenocarcinoma cells, Mol. Carcinog. 53 (2014) 659–666.
[27] K. Mihara, R. Ramachandran, M. Saifeddine, K.K. Hansen, B. Renaux, D. Polley, S. Gibson, C. Vanderboor, M.D. Hollenberg, Thrombin-mediated direct activation of proteinase-activated Receptor-2: another target for thrombin signaling, Mol. Pharmacol. 89 (2016) 606–614.
[28] C. Ay, D. Dunkler, R. Simanek, J. Thaler, S. Koder, C. Marosi, C. Zielinski, I. Pabinger, Prediction of venous thromboembolism in patients with cancer by measuring thrombin generation: results from the Vienna Cancer and Thrombosis Study, J. Clin. Oncol. 29 (2011) 2099–2103.
[29] M.S. Park, B.A. Owen, B.A. Ballinger, M.G. Sarr, H.J. Schiller, S.P. Zietlow,

D.H. Jenkins, M.H. Ereth, W.G. Owen, J.A. Heit, Quantification of hypercoagulable state after blunt trauma: microparticle and thrombin generation are increased relative to injury severity, while standard markers are not, Surgery 151 (2012) 831–836.
[30] I. Jahan, J. Fujimoto, S.M. Alam, E. Sato, T. Tamaya, Role of protease activated receptor-2 in lymph node metastasis of uterine cervical cancers, BMC Cancer 8 (2008) 301.
[31] E. Jin, M. Fujiwara, X. Pan, M. Ghazizadeh, S. Arai, Y. Ohaki, K. Kajiwara, T. Takemura, O. Kawanami, Protease-activated receptor (PAR)-1 and PAR-2 participate in the cell growth of alveolar capillary endothelium in primary lung adenocarcinomas, Cancer 97 (2003) 703–713.
[32] I. Jahan, J. Fujimoto, S.M. Alam, E. Sato, H. Sakaguchi, T. Tamaya, Role of protease activated receptor-2 in tumor advancement of ovarian cancers, Ann. Oncol. 18 (2007) 1506–1512.
[33] N. Michel, N. Heuze-Vourc'h, E. Lavergne, C. Parent, M.L. Jourdan, A. Vallet, S. Iochmann, O. Musso, P. Reverdiau, Y. Courty, Growth and survival of lung cancer cells: regulation by kallikrein-related peptidase 6 via activation of proteinase-activated receptor 2 and the epidermal growth factor receptor, Biol. Chem. 395 (2014) 1015–1025.
[34] S.H. Huang, Y. Li, H.G. Chen, J. Rong, S. Ye, Activation of proteinase-activated receptor 2 prevents apoptosis of lung cancer cells, Cancer Investig. 31 (2013) 578–581.
[35] L. Yang, Y. Ma, W. Han, W. Li, L. Cui, X. Zhao, Y. Tian, Z. Zhou, W. Wang, H. Wang, Proteinase-activated receptor 2 promotes cancer cell migration through RNA methylation-mediated repression of miR-125b, J. Biol. Chem. 290 (2015) 26627–26637.
[36] S. Lamouille, J. Xu, R. Derynck, Molecular mechanisms of epithelial-mesenchymal transition, Nat. Rev. Mol. Cell Biol. 15 (2014) 178–196.
[37] C.W. Liu, C.H. Li, Y.J. Peng, Y.W. Cheng, H.W. Chen, P.L. Liao, J.J. Kang, M.H. Yeng, Snail regulates Nanog status during the epithelial-mesenchymal transition via the Smad1/Akt/GSK3beta signaling pathway in non-small-cell lung cancer, Oncotarget 5 (2014) 3880–3894.
[38] T.Y. Chou, W.C. Chen, A.C. Lee, S.M. Hung, N.Y. Shih, M.Y. Chen, Clusterin silencing in human lung adenocarcinoma cells induces a mesenchymal-to-epithelial transition through modulating the ERK/Slug pathway, Cell. Signal. 21 (2009) 704–711.
[39] J. Qu, M. Li, J. An, B. Zhao, W. Zhong, Q. Gu, L. Cao, H. Yang, C. Hu, MicroRNA-33b inhibits lung adenocarcinoma cell growth, invasion, and epithelial-mesenchymal transition by suppressing Wnt/beta-catenin/ZEB1 signaling, Int. J. Oncol. 47 (2015) 2141–2152.
[40] K. Pallier, A. Cessot, J.F. Côté, P.A. Just, A. Cazes, E. Fabre, C. Danel, M. Riquet, M. Devouassoux-Shisheboran, S. Ansieau, A. Puisieux, P. Laurent-Puig, H. Blons, TWIST1 a new determinant of epithelial to mesenchymal transition in EGFR mutated lung adenocarcinoma, PLoS One 7 (2012) e29954.
[41] H.J. Zhang, H.Y. Wang, H.T. Zhang, J.M. Su, J. Zhu, H.B. Wang, W.Y. Zhou, H. Zhang, M.C. Zhao, L. Zhang, X.F. Chen, Transforming growth factor-beta1 promotes lung adenocarcinoma invasion and metastasis by epithelial-to-mesenchymal transition, Mol. Cell. Biochem. 355 (2011) 309–314.
[42] J.S. Song, C.M. Kang, C.K. Park, H.K. Yoon, Thrombin induces epithelial-mesenchymal transition via PAR-1, PKC, and ERK1/2 pathways in A549 cells, Exp. Lung Res. 39 (2013) 336–348.
[43] S. Ando, H. Otani, Y. Yagi, K. Kawai, H. Araki, S. Fukuhara, C. Inagaki, Proteinase-activated receptor 4 stimulation-induced epithelial-mesenchymal transition in alveolar epithelial cells, Respir. Res. 8 (2007) 31.
[44] M. Wygrecka, M. Didiasova, S. Berscheid, K. Piskulak, B. Taborski, D. Zakrzewicz, G. Kwapiszewska, K.T. Preissner, P. Markart, Protease-activated receptors (PAR)-1 and -3 drive epithelial-mesenchymal transition of alveolar epithelial cells - potential role in lung fibrosis, Thromb. Haemost. 110 (2013) 295–307.
[45] X. Su, E. Camerer, J.R. Hamilton, S.R. Coughlin, M.A. Matthay, Protease-activated receptor-2 activation induces acute lung inflammation by neuropeptide-dependent mechanisms, J. Immunol. 175 (2005) 2598–2605.
[46] M.C. Winter, S.S. Shasby, D.R. Ries, D.M. Shasby, PAR2 activation interrupts E-cadherin adhesion and compromises the airway epithelial barrier: protective effect of beta-agonists, Am. J. Phys. Lung Cell. Mol. Phys. 291 (2006) L628–L635.
[47] S.C. Lin, Y.T. Chou, S.S. Jiang, J.L. Chang, C.H. Chung, Y.R. Kao, I.S. Chang, C.W. Wu, Epigenetic switch between SOX2 and SOX9 regulates cancer cell plasticity, Cancer Res. 76 (2016) 7036–7048.
[48] C.H. Huang, W.H. Yang, S.Y. Chang, S.K. Tai, C.H. Tzeng, J.Y. Kao, K.J. Wu, M.H. Yang, Regulation of membrane-type 4 matrix metalloproteinase by SLUG contributes to hypoxia-mediated metastasis, Neoplasia 11 (2009) 1371–1382.
[49] S.J. Mansour, J.M. Candia, K.K. Gloor, N.G. Ahn, Constitutively active mitogen-activated protein kinase kinase 1 (MAPKK1) and MAPKK2 mediate similar transcriptional and morphological responses, Cell Growth Differ. 7 (1996) 243–250.
[50] C.D. Wells, M.Y. Liu, M. Jackson, S. Gutowski, P.M. Sternweis, J.D. Rothstein, T. Kozasa, P.C. Sternweis, Mechanisms for reversible regulation between G13 and Rho exchange factors, J. Biol. Chem. 277 (2002) 1174–1181.
[51] R. Tsutsumi, H. Higashi, M. Higuchi, M. Okada, M. Hatakeyama, Attenuation of *Helicobacter pylori* CagA × SHP-2 signaling by interaction between CagA and C-terminal Src kinase, J. Biol. Chem. 278 (2003) 3664–3670.
[52] R. Somwar, S. Koterski, G. Sweeney, R. Sciotti, S. Djuric, C. Berg, J. Trevillyan, P.E. Scherer, C.M. Rondinone, A. Klip, A dominant-negative p38 MAPK mutant and novel selective inhibitors of p38 MAPK reduce insulin-stimulated glucose uptake in 3T3-L1 adipocytes without affecting GLUT4 translocation, J. Biol. Chem. 277 (2002) 50386–50395.
[53] S. Ahn, H. Wei, T.R. Garrison, R.J. Lefkowitz, Reciprocal regulation of angiotensin receptor-activated extracellular signal-regulated kinases by beta-arrestins 1 and 2, J. Biol. Chem. 279 (2004) 7807–7811.
[54] C.C. Tsai, T.Y. Kuo, Z.W. Hong, Y.C. Yeh, K.S. Shih, S.Y. Du, H.W. Fu, *Helicobacter pylori* neutrophil-activating protein induces release of histamine and interleukin-6 through G protein-mediated MAPKs and PI3K/Akt pathways in HMC-1 cells, Virulence 6 (2015) 755–765.
[55] Y.W. Chu, P.C. Yang, S.C. Yang, Y.C. Shyu, M.J. Hendrix, R. Wu, C.W. Wu, Selection of invasive and metastatic subpopulations from a human lung adenocarcinoma cell line, Am. J. Respir. Cell Mol. Biol. 17 (1997) 353–360.
[56] S.J. Compton, S. Sandhu, S.J. Wijesuriya, M.D. Hollenberg, Glycosylation of human proteinase-activated receptor-2 (hPAR2): role in cell surface expression and signalling, Biochem. J. 368 (2002) 495–505.
[57] M.N. Adams, C.N. Pagel, E.J. Mackie, J.D. Hooper, Evaluation of antibodies directed against human protease-activated receptor-2, Naunyn Schmiedeberg's Arch. Pharmacol. 385 (2012) 861–873.
[58] T. Kozasa, X. Jiang, M.J. Hart, P.M. Sternweis, W.D. Singer, A.G. Gilman, G. Bollag, P.C. Sternweis, p115 RhoGEF, a GTPase activating protein for Galpha12 and Galpha13, Science 280 (1998) 2109–2111.
[59] S. Su, Y. Li, Y. Luo, Y. Sheng, Y. Su, R.N. Padia, Z.K. Pan, Z. Dong, S. Huang, Proteinase-activated receptor 2 expression in breast cancer and its role in breast cancer cell migration, Oncogene 28 (2009) 3047–3057.
[60] V. Stambolic, J.R. Woodgett, Mitogen inactivation of glycogen synthase kinase-3 beta in intact cells via serine 9 phosphorylation, Biochem. J. 303 (Pt 3) (1994) 701–704.
[61] M. Medina, F. Wandosell, Deconstructing GSK-3: the fine regulation of its activity, Int. J. Alzheimers Dis. 2011 (2011) 479249.
[62] Q. Ding, W. Xia, J.C. Liu, J.Y. Yang, D.F. Lee, J. Xia, G. Bartholomeusz, Y. Li, Y. Pan, Z. Li, R.C. Bargou, J. Qin, C.C. Lai, F.J. Tsai, C.H. Tsai, M.C. Hung, Erk associates with and primes GSK-3beta for its inactivation resulting in upregulation of beta-catenin, Mol. Cell 19 (2005) 159–170.
[63] T.M. Thornton, G. Pedraza-Alva, B. Deng, C.D. Wood, A. Aronshtam, J.L. Clements, G. Sabio, R.J. Davis, D.E. Matthews, B. Doble, M. Rincon, Phosphorylation by p38 MAPK as an alternative pathway for GSK3beta inactivation, Science 320 (2008) 667–670.
[64] A.V. Bakin, A.K. Tomlinson, N.A. Bhowmick, H.L. Moses, C.L. Arteaga, Phosphatidylinositol 3-kinase function is required for transforming growth factor beta-mediated epithelial to mesenchymal transition and cell migration, J. Biol. Chem. 275 (2000) 36803–36810.
[65] Y. Zhao, H. Wang, X. Li, M. Cao, H. Lu, Q. Meng, H. Pang, H. Li, C. Nadolny, X. Dong, L. Cai, Ang II-AT1R increases cell migration through PI3K/AKT and NF-kappaB pathways in breast cancer, J. Cell. Physiol. 229 (2014) 1855–1862.
[66] J. Chen, J.K. Chen, R.C. Harris, Angiotensin II induces epithelial-to-mesenchymal transition in renal epithelial cells through reactive oxygen species/Src/caveolin-mediated activation of an epidermal growth factor receptor-extracellular signal-regulated kinase signaling pathway, Mol. Cell. Biol. 32 (2012) 981–991.
[67] Z. Xu, L. Zhu, M. Yao, G. Zhong, Q. Dong, A. Yu, PTEN plays an important role in thrombin-mediated lung cancer cell functions, Biomed. Res. Int. 2015 (2015) 459170.
[68] S. Rajagopal, K. Rajagopal, R.J. Lefkowitz, Teaching old receptors new tricks: biasing seven-transmembrane receptors, Nat. Rev. Drug Discov. 9 (2010) 373–386.
[69] K.J. Svensson, P. Kucharzewska, H.C. Christianson, S. Sköld, T. Löfstedt, M.C. Johansson, M. Morgelin, J. Bengzon, W. Ruf, M. Belting, Hypoxia triggers a proangiogenic pathway involving cancer cell microvesicles and PAR-2-mediated heparin-binding EGF signaling in endothelial cells, Proc. Natl. Acad. Sci. U. S. A. 108 (2011) 13147–13152.
[70] H.H. Versteeg, F. Schaffner, M. Kerver, L.G. Ellies, P. Andrade-Gordon, B.M. Mueller, W. Ruf, Protease-activated receptor (PAR) 2, but not PAR1, signaling promotes the development of mammary adenocarcinoma in polyoma middle T mice, Cancer Res. 68 (2008) 7219–7227.
[71] L. Ge, S.K. Shenoy, R.J. Lefkowitz, K. DeFea, Constitutive protease-activated receptor-2-mediated migration of MDA MB-231 breast cancer cells requires both beta-arrestin-1 and -2, J. Biol. Chem. 279 (2004) 55419–55424.
[72] X. Zhang, F. Wang, X. Chen, J. Li, B. Xiang, Y.Q. Zhang, B.M. Li, L. Ma, Beta-arrestin1 and beta-arrestin2 are differentially required for phosphorylation-dependent and -independent internalization of delta-opioid receptors, J. Neurochem. 95 (2005) 169–178.
[73] F.T. Kuo, T.L. Lu, H.W. Fu, Opposing effects of beta-arrestin1 and beta-arrestin2 on activation and degradation of Src induced by protease-activated receptor 1, Cell. Signal. 18 (2006) 1914–1923.
[74] A. Vibhuti, K. Gupta, H. Subramanian, Q. Guo, H. Ali, Distinct and shared roles of beta-arrestin-1 and beta-arrestin-2 on the regulation of C3a receptor signaling in human mast cells, PLoS One 6 (2011) e19585.
[75] H. Ueda, R. Morishita, J. Yamauchi, H. Itoh, K. Kato, T. Asano, Regulation of Rac and Cdc42 pathways by G(i) during lysophosphatidic acid-induced cell spreading, J. Biol. Chem. 276 (2001) 6846–6852.
[76] C.C. Yang, L.D. Hsiao, C.M. Yang, C.C. Lin, Thrombin enhanced matrix metalloproteinase-9 expression and migration of SK-N-SH cells via PAR-1, c-Src, PYK2, EGFR, Erk1/2 and AP-1, Mol. Neurobiol. 54 (2017) 3476–3491.